Variable Noise Reduction Systems for a Notional Supersonic Business Jet

Jeffrey J. Berton*
NASA Glenn Research Center, Cleveland, Ohio 44135

A variable noise reduction system consists of equipment on board an airplane that is designed to reduce noise in the vicinity of airports. They are anticipated to be used on supersonic civil aircraft currently under development by industry. They are investigated in this paper for a notional 55-tonne supersonic business jet. The airplane concept was developed by NASA for use in environmental impact studies conducted by the International Civil Aviation Organization. The variable noise reduction system investigated implements a programmed thrust lapse procedure and a programmed flap retraction procedure. The procedures are expected to reduce noise in aircraft certification as well as in operational practice. Behavior of the aircraft in a noise certification setting is considered. Variables of the procedures are optimized to reduce noise levels. Certification considerations unique to these systems are discussed for transport-category large airplanes and jet-powered airplanes. A novel method for evaluating lateral noise is used.

I. Introduction

SUPERSONIC Technology Concept Aeroplanes† are conceptual research vehicles studied with the intent to provide information to the International Civil Aviation Organization by way of their Committee on Aviation Environmental Protection (CAEP). Though several STCAs have been investigated by CAEP, the focus of this paper is an analysis of an eight-passenger supersonic business jet developed by NASA. The airplane is intended to be generally representative of early market entrant supersonic business jet aircraft being considered by industry. It is designed to travel transatlantic distances at Mach 1.4 using relatively near-term technologies. It is equipped with conceptual engines designed and assessed by NASA. They are derived from the core of a contemporary, "off-the-shelf" subsonic turbofan. All aspects of the airplane and engine have been developed entirely with information from the public domain. Being nonproprietary and transparent, the STCA is ideal for use in ICAO's public studies. Aircraft mission performance, airport-vicinity noise, and exhaust emissions are predicted for the STCA using NASA tools.

NASA began work on the STCA in 2017 in support of ICAO. By the following year, CAEP proposed to conduct an exploratory study on the global impact of future civil supersonic aircraft. The study was approved at CAEP's eleventh triennial meeting in 2019 [1]. The FAA endorsed the study [2] and requested that NASA assist it by providing the STCA's performance, fuel burn, noise, and exhaust emission data. The study predicted the outcome of adding supersonic transports to the existing civil aircraft fleet. The study was part of the work program of CAEP's twelfth (previous) program cycle and has since been completed. The STCA was an analytical proxy for future supersonic business jet types. The influence that supersonic airplanes are expected to have on operations, fuel consumption, airport noise, and air quality were assessed. Since then, the STCA continues to serve as a notional reference airplane used in studies conducted by NASA [3-5] and by others [6-13]. This paper documents an additional NASA study using the STCA.

In general, a *variable noise reduction system* (VNRS) consists of onboard equipment that changes the operating condition or the configuration of an airplane [14]. A VNRS is intended to be permanent, integral equipment that engages without the need of flight crew activation (as opposed to a *selectable noise reduction system*, which must be activated by the flight crew). A VNRS engages automatically with every operation, though if necessary it could be designed to be overridden in some emergency situations. Activation of these systems causes preprogrammed procedures to be implemented that reduce noise in some manner. These systems are intended to work in noise certification as well as in normal operational practice. A VNRS provision exists for rotorcraft [15], but as yet none have been defined for transport-category large airplanes and jet-powered airplanes.

---

*Aerospace Engineer, Propulsion Systems Analysis Branch, senior member AIAA.

†In referring to STCAs, "aeroplane" is the spelling used by ICAO. The spelling "airplane," however, is used in this paper.

In previous NASA studies, the STCA relied on just one VNRS procedure known as a programmed thrust lapse, or a programmed lapse rate (PLR) procedure. The PLR procedure reported in [4] was not optimized. In this paper, programmable flaps are investigated as a second, additional VNRS procedure. Taken together and with optimization, the systems are predicted to reduce noise of the STCA on a cumulative basis by an additional 5.2 EPNdB relative to the higher levels reported previously [4].

A novel VNRS noise modeling method unique to transport-category large airplanes and jet-powered airplanes is proposed in this paper. Certification considerations of these systems are discussed. The behavior of the aircraft in a noise certification setting is considered. Behavior of the aircraft in an operational setting is investigated in a companion paper [16].

In places throughout this paper, commentary is given on the differences and needs of supersonic civil airplanes relative to subsonic airplanes, particularly in the terminal airspace where they intermingle. NASA does not presume the need for, or prejudge the design of new regulatory standards and recommended practices for supersonic transports. Instead, the comments should be viewed as benign technical observations regarding the needs of its own notional STCA.

II. Airframe and engines

Prerequisites for computing takeoff performance and noise data are working multidisciplinary models for the vehicle. Weight, aerodynamics, and propulsion analyses taken from [4] are described in the following sections.

A. Concept airframe

The STCA is a notional, eight-passenger business jet designed for Mach 1.4 supersonic overwater cruise speeds. It has a low-aspect ratio cranked delta wing. Three engines are mounted aft; the outboard engines are mounted on short fuselage pylons, while the center engine is integrated with the vertical tail. A summary of vehicle characteristics is shown in Table 1. A solid model of the airplane is shown in Figure 1.

The airplane has no features that would reduce its sonic boom noise signature, making it similar in that respect to other early market entrant designs. Supersonic speeds over land would be restricted where prohibited. Despite NASA's current interest in low-boom supersonic aircraft [17], those types of designs are viewed here as candidates for later markets.

Table 1: STCA characteristics.

Max takeoff weight, klb	121
Passengers	8
Cruise Mach	1.4
Overall length, ft	135
Span, ft	67
Wing reference area, ft^2	1619
Wing aspect ratio	2.7
Wing taper ratio	0.09
Wing loading, lb/ft^2	74
Wing fuel, klb	24
Fuselage fuel, klb	36
Fuel fraction	0.50

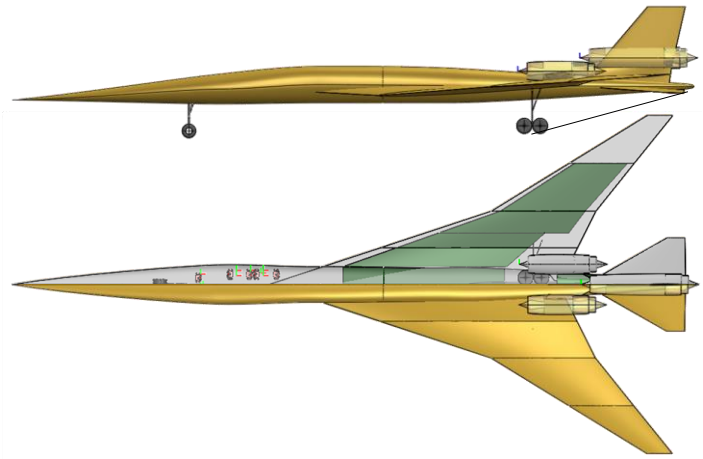

Figure 1. Solid model of the STCA.

Several aircraft conceptual design tools are used to synthesize the vehicle. A solid modeling tool [18] is used to define the outer mold lines of the airplane, to guide interior packaging, and to estimate internal fuel volume. The solid model also informs component weight and vehicle aerodynamic analyses. Lift-dependent drags, lift-independent drags, and wave drags are calculated by the methods described in Refs. [19-21]. A weight estimate of the wing is made using physics-based factors based on its gross geometry, while weight estimates of other major structures and systems are made using statistical-empirical relations. All airframe weight estimation methods are discussed in [22]. These computer codes are organized together using a frameworking tool [23] which provides a conceptual-level, multidisciplinary, integrated process for designing and analyzing supersonic aircraft [24]. Using this integrated design

environment, major aircraft design variables can be rapidly assessed and optimized. A design and sizing analysis of wing, fuselage and tail characteristics is performed, subject to practical performance constraints.

The vehicle design is optimized to maximize range for a fixed maximum gross weight of 55t (121klb). Subject to a minimum cabin width of 7ft, fuselage section height, width, and tangent angles at three stations are optimized to minimize wave drag. Wing planform shape, airfoil twist, and camber are varied to minimize wave drag and lift-dependent drag. Horizontal tail size and location, main gear location, and trailing edge and leading edge flap deflections are optimized to meet takeoff, landing, and cruise static margin constraints, and to ensure reasonable takeoff and landing field lengths and approach velocity.

B. Propulsion

For an early market entrant, it is unlikely that a completely new engine could be developed and be ready in time for a near-term entry into service. Instead, it is more likely that the low-pressure spool of a contemporary off-the-shelf engine would be redesigned and repurposed, resulting in a supersonic variant of an existing subsonic turbofan. In this study, an analytical model of a subsonic CFM International CFM56-7B27 is used as the "donor" engine from which the supersonic engine is derived. Interestingly, the original CFM56-2, granted certification in 1979, was itself derived from the General Electric F101 model used for the supersonic B-1A bomber. Redesigning the low-pressure spool of a CFM56 once again for a supersonic application would bring the engine family full circle.

Because much engine design data are closely-held, proprietary, and unavailable, any analytic simulation of a CFM56 (outside of CFM International) will necessarily have some inherent inaccuracy. Nevertheless, if data can be obtained from public-domain sources (such as type certificate data sheets, manufacturer-provided operating documents, technical reports, and manufacturer's websites), simulations of turbofans developed outside of engine companies can be reasonably accurate. A model of the subsonic CFM56 is created with such information using the Numerical Propulsion System Simulation code (NPSS, [25, 26]) to predict engine performance. The subsonic CFM56 model is adapted from work performed under the FAA's Environmental Design Space initiative [27, 28].

The low-pressure spool of the CFM56-7B is redesigned for a Mach 1.4 cruise application. The booster is discarded (with it, supersonic ram effects would elevate aft stages of the compressor to excessive temperature), and the fan and low-pressure turbine are redesigned for a higher pressure ratio. Fan performance is modeled using data collected at NASA from the GE57 scale model fan [29]. The GE57 fan is considered to be perhaps representative of what might be used by an engine manufacturer in a supersonic refan application. It consists of a single stage and operates at peak efficiency at a pressure ratio of 2.2. Fan pressure ratio is a design variable strongly influencing engine performance. A high fan pressure ratio is preferred to create an exhaust velocity high enough for supersonic flight, while a low fan pressure ratio is required to meet takeoff and landing noise requirements. Fan pressure ratio, along with a practical extraction ratio, directly determine the bypass ratio of the engine. This poses conflicting requirements for supersonic engine designers. If fan pressure ratios are high enough, they could lead to supercritical nozzle pressure ratios at low altitude and create high levels of jet shock cell noise during takeoff.

Another design choice is whether to forcibly mix the core and bypass streams or to allow them to remain separate. There are compelling reasons to mix the streams. There is usually an increase in gross thrust when flows are forcibly mixed and exhausted through a common nozzle, with the benefit increasing with increasing core stream temperature. And the outer mold lines of a simpler, single-stream nozzle are preferred over those of a more complex coannular nozzle if sonic boom reduction is important. In this study, core and bypass streams are forcibly mixed through a lobed mixer. The design extraction ratio is kept near unity so that mixer bypass port and mixer exit Mach numbers are always less than 0.5.

The mixed flow exits through a single-stream convergent-divergent plug nozzle. The centerbody plug and nozzle throat are fixed while the divergent flaps are variable. The plug is important in keeping aftbody boattail angles small during supersonic cruise while also lowering takeoff jet noise slightly. At low altitudes, the divergent nozzle flaps are closed to a minimum area so that the nozzle exit plane is the throat. Solid models of the CFM56-7B and the derived supersonic variant are shown in Figure 2. Not shown in the figure are the nozzles or inlets for either engine.

At the cycle design point, characteristics of the compressor and the high-pressure turbine are set manually to those of the CFM56 donor engine. This keeps the high-pressure spool of the supersonic derivative engine identical to the CFM56 core. Bleed flow fractions and core flow passage areas are also held constant. Hot section temperatures are kept nearly as high as the CFM56 maximum takeoff temperatures. But since the supersonic variant would spend several hours at maximum temperature (compared to just a few minutes during takeoff for a subsonic turbofan), this becomes a rather important assumption. Maintaining high temperatures is justified by assuming increased hot section overhaul frequency (not uncommon for a business jet application), and perhaps by offering new turbine airfoils with improved materials, coatings, and better cooling effectiveness.

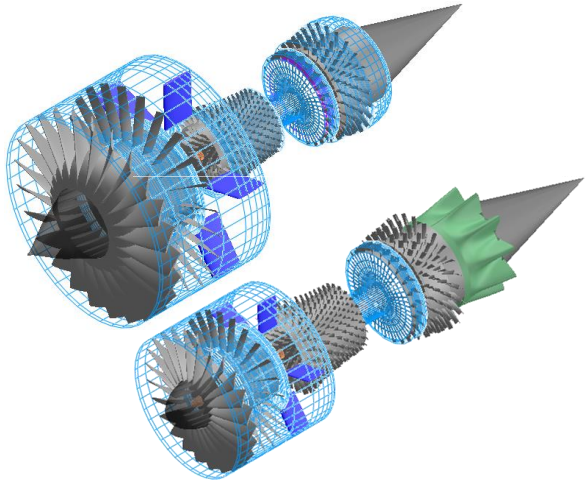

Figure 2. Solid models of the CFM56-7B (top) and conceptual modified supersonic variant (bottom).

Fan pressure ratios are selected such that the nozzle operates on the cusp of choke near sea level. With a small amount of engine derating at low altitude, jet shock cell noise is eliminated during takeoff. A summary of engine performance data is shown in Table 2. Ambient conditions above 10,000 feet use International Standard Atmosphere (ISA) conditions, while conditions nearer sea level use hot day (ISA+27°F) conditions. Performance data at sea level are shown after engine derating. Additional information for the STCA equipped with these engines is available in [4].

Table 2. Performance summary for the STCA engine.

	M1.4, 50kft, ISA	M0.25, sea level, ISA+27°F	Sea level static, ISA+27°F
Net thrust, lb/engine	3330	14,140	16,620
Specific fuel consumption, lb/hr/lb	0.943	0.588	0.479
Bypass ratio	2.9	2.9	3.0
Burner temperature, °R	3300	3150	3130
Turbine inlet temperature, °R	3180	3040	3020
Compressor exit temperature, °R	1450	1440	1430
Overall pressure ratio	22	21	21
Fan pressure ratio	2.0	1.9	1.9
Compressor pressure ratio	11.2	11.1	11.2
Extraction ratio	1.1	1.1	1.1
Nozzle pressure ratio	5.9	1.9	1.8

C. Mission performance

With aerodynamics, engine thrust and fuel consumption performance known, a mission analysis of the transport can be made using NASA mission performance software [30]. The design mission is at maximum takeoff gross weight, with a single cruise segment at supersonic speed. There are no subsonic cruise segments which might be typical of other missions where supersonic flight might be restricted. Since high-altitude air traffic should be light, block altitude clearance is assumed and the airplane is allowed to climb continuously during supersonic cruise. The design mission uses the full payload complement of eight passengers. The mission rules described in [31] are followed, except that the five percent block fuel reserve allowance is omitted, which is more typical of mission rules followed by business jets. The mission profile is shown in Figure 3. The design mission range of the STCA is 4243nmi. Performance results are shown in Table 3.

Table 3: STCA performance.

Takeoff gross wt, klb	121
Operating empty wt, klb	51
Payload, lb	1640
Climb time, min	47
Cruise altitude, kft	44-51
Cruise lift-drag ratio	6.6-7.9
Block time, hr	5.9
Block fuel, klb	61
Reserve fuel, klb	8
Range, nmi	4243

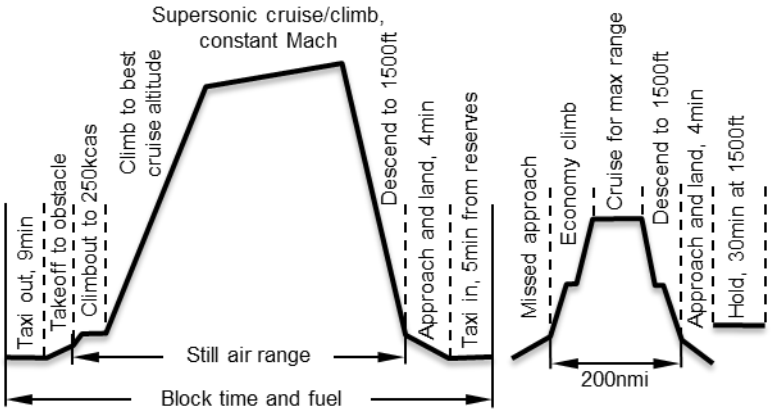

Figure 3. STCA mission profile.

III. Variable noise reduction systems

Except for the Aérospatiale/BAC Concorde, regulations [32, 33] do not include noise standards for supersonic airplanes. But several U.S. manufacturers are promising to build and certify new supersonic civil aircraft, and the FAA's legal interpretation of their statutory duty [34] obliges the agency to create new noise standards for them. These standards are necessary to provide regulatory certainty for manufacturers and other aviation stakeholders.

To this end, the FAA issued a notice of proposed rulemaking for landing and takeoff noise standards of new supersonic aircraft in April, 2020 [35]. The FAA's intention is to revise its noise standards to include provisions for future supersonic transports. The proposed rulemaking clarifies that a VNRS (recognized previously for rotorcraft) could be used for noise certification testing of new supersonic transports. While not requiring any specific VNRS for supersonic types, the proposed rulemaking makes clear that they are optional innovations for manufacturers. In this study, and commensurate with the guidance in [35], the noise standards and recommended practices for large subsonic transport-category and subsonic jet-powered airplanes are assumed to apply broadly to future supersonic transports. Further, use of a VNRS as recommended in [35] is assumed to apply broadly to the STCA. And though an automatic flap retraction system is not mentioned explicitly in [35], it is assumed that such a system can be combined with an automatic thrust reduction system as a single VNRS for the STCA. In research performed during NASA's High Speed Research Program, these procedures were generally accepted by pilots conducting simulated takeoffs, and no obvious safety issues were discovered [36].

A. Programmed lapse rate procedure

Noise, of course, is a strong function of engine power setting. So during noise certification, applicants are motivated to use no more engine power than is necessary. But unless approved otherwise, or unless engine power is part of a VNRS, actively manipulating engine power is restricted by Annex 16 noise regulations [32]. Section 3.6.2 of the Annex requires that maximum takeoff thrust be maintained until the airplane reaches various minimum safe altitudes dependent upon the number of engines. And ordinarily for an airplane in this category, the only change to engine thrust permitted during its takeoff reference procedure is the pilot-initiated engine power cutback. Without permission to operate otherwise or unless an approved VNRS is involved, regulations rule out part-power takeoffs for noise certification and they would seem also to disallow any type of "thrust lapse" procedure at low altitude. Further, regulating authorities might be reluctant to approve a pilot-initiated procedure that would increase the workload of the flight crew during takeoff and reduce the rate of climb.

Still, in the interest of noise reduction, it is thought that a departure from normal reference procedures could be permitted if computer-controlled automatic throttle scheduling is used, making pilot initiation unnecessary. An automatic digital engine control implementation of a programmed thrust lapse could use an airplane's weight-on-wheels sensors, airspeed, altimeter, attitude and air temperature indicators, or perhaps airport navigational aids to begin preprogrammed thrust reduction.

Thus, it is anticipated that a PLR procedure would be classified as a VNRS so that it could comply readily with existing standards. When an airplane is equipped with an approved VNRS that would prevent compliance with normal reference procedures, a departure from them may be approved by the certifying authority. For large, transport-category and jet-powered airplane types, these conditions are discussed in Section 3.6.1.4 of [32].

Supersonic transports in particular are expected to benefit from PLR procedures. Experience in aircraft sizing suggests that supersonic aircraft are likely to be constrained by a takeoff field distance requirement. Therefore, high engine power settings are required during the ground roll and climbout phases of takeoff. But engines capable of supersonic cruise tend to have high specific thrust, high exhaust velocity, and high levels of jet noise, making noise certification a challenging prospect. Reducing jet noise at the lateral measurement condition, where engine power is maximum, is particularly challenging (a sketch showing the arrangement of the noise measurement monitors is shown in Figure 4). In the 1970s, the FAA speculated [37] on the regulatory aspects of programmed takeoff throttle schedules for supersonic transports. Around the same time, researchers in NASA's Supersonic Cruise Research Program proposed an automatic thrust lapse procedure [38] to address noise at the lateral condition. This procedure since has become known as the auto-throttle or the PLR procedure takeoff [39].

As typically envisioned, a takeoff using a PLR procedure begins ordinarily, with maximum thrust applied from brake release through rotation and liftoff. Propulsion noise is of course highest at maximum thrust, but for observers located laterally across from the aircraft, noise is very efficiently attenuated by ground effects. Lateral attenuation is caused by ground surface absorption, by atmospheric refraction and scattering effects, and by engine-airframe installation effects. At low elevation angles, these effects can attenuate sound along the lateral sideline by as much as 10dB [40-43]. The PLR procedure exploits lateral attenuation.

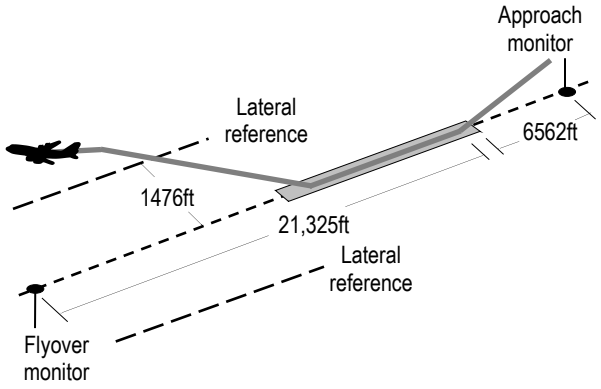

Figure 4. Noise certification monitor arrangement relative to takeoff and landing flight paths.

Soon after the runway obstacle is cleared (but before the conventional, pilot-initiated thrust cutback takes place), thrust is automatically lowered to reduce lateral sideline noise. The programmed thrust lapse might be more gradual than the rather abrupt pilot-initiated thrust cutback occurring later. Ideally, engine thrust is reduced as the benefit of lateral attenuation vanishes with increasing altitude.

Thus, capitalizing on lateral attenuation via a thrust lapse procedure is a clever idea. Lateral noise is abated, but because takeoff thrust is at maximum from brake release through the 35-foot runway obstacle, the takeoff field length does not increase. In the previous STCA study [4], a simple 10 percent PLR was implemented approximately over the time required for gear retraction, and it was completed before the second segment climb began. No optimization of the PLR procedure was considered. In this study, a more precise definition of the procedure (i.e., how much thrust is allowed to lapse and when it begins and ends) using optimization is investigated.

B. Programmed flap retraction procedure

A review of flap systems used in previous civil supersonic transports is not particularly helpful. The Aérospatiale/BAC Concorde was not equipped with high-lift devices. Its elevons were used for trim and control only. Nor did the Tupolev Tu-144 employ high-lift devices on its main delta wing, though in production versions its canard had retractable leading- and trailing-edge flaps. The Concorde and the Tu-144 had relatively poor low-speed performance compared to similarly-sized subsonic aircraft. Both of them employed afterburners to help shorten their takeoff field distance and to improve their rates of climb.

But like many subsonic aircraft, it is anticipated that future supersonic civil aircraft will be equipped with high-lift devices to improve low-speed performance during takeoff and landing [44]. Indeed, NASA's STCA is equipped with leading- and trailing-edge flaps. These are considered necessary additions since (unlike the Concorde and the Tu-144) excessive noise precludes afterburning as a solution to its low-speed performance problem. The STCA's trailing-edge plain flaps and leading-edge "droop nose" flaps are modeled as simple, hinged devices without slotted gaps to help control flow. Such devices increase local camber, but they do not extend the wing chord. These arrangements are simple and rigid. And since they need not occupy much wing volume, they are well-suited for use in thin, supersonic wings. Both systems can be controlled by torque tube motors located within the fuselage.

Like the PLR procedure, manipulating high-lift devices during the takeoff reference procedure has regulatory implications. Unless permission is granted to operate otherwise, Section 3.6.2(e) of [32] states that – except for landing gear retraction – a vehicle configuration selected by the applicant must be maintained throughout the procedure. This is required so that the noise signature during the measurement period is not complicated by extraneous effects. It is

clarified in the section that lift augmentation devices are among the items meant by "configuration." But much like the PLR procedure, a flap retraction sequence could be programmed, automated, and classified as a VNRS. Such a VNRS would ordinarily prevent compliance with normal reference procedures, but if approved by a certifying authority, a departure from them could be allowed under Section 3.6.1.4 of [32]. Automatic flap retraction systems for noise certification were planned for the High-Speed Civil Transport [36, 45], and were reportedly considered for Aerion's AS2 supersonic business jet [46].

All of this of course is in sharp contrast with ordinary operational practice, where flaps and slats are retracted on appropriate, sensible schedules during climbout. Optimal flap retraction schedules for the STCA in an operational setting were defined by NASA and were used by CAEP in their supersonic exploratory study [1]. Operational noise abatement departure profiles for the STCA are reported in the companion paper [16].

In the previous STCA study [4], a programmed flap retraction procedure was not considered for noise certification predictions. Two takeoff procedures were defined for the STCA: a minimum field distance procedure and a delayed rotation procedure. For both cases, a flap study was performed to determine optimal flap deflection angles. The delayed rotation procedure was used to calculate the takeoff reference profile for noise certification predictions, and it is developed further in this paper.

In the previous study [4], flap deflections for the delayed rotation procedure were selected not only with field distance and initial climb rate in mind, but also with noise certification. Flap deflection influences how much the engine thrust can be cut back per 3.6.2(b) of [32], and therefore it is an important factor in noise measured at the flyover monitor. Fixed leading edge and trailing edge flap deflections were selected via a parametric study for a combination of good field performance, climb rate, and low pilot-initiated cutback thrust (6deg. and 10deg., respectively). These deflections were maintained throughout the takeoff reference procedure. Thus, the flap setting selected was a compromise. Relatively high flap deflections are preferred to improve lift, to lower rotation speed and liftoff speed, and to reduce takeoff field distance. But after the airplane has accelerated and after it is aloft, a clean configuration is preferred so that the airplane can enjoy better lift-drag ratios and higher climb rates. Flap retraction has the beneficial effect of increasing altitude over the flyover noise monitor and reducing flyover noise. Unlike the previous study [4], the takeoff reference profile in this study includes an optimized flap retraction schedule controlled by a VNRS.

C. Acceleration procedure

There is little point in retracting flaps unless the airplane has reached an airspeed that is appropriate for a clean configuration. High-lift devices are effective in increasing lift, lowering the so-called airworthiness V-speeds, and for improving takeoff field distance. But once aloft and once airspeed is high enough to reduce the required lift coefficient, a clean configuration is preferred so that a higher lift-to-drag ratio can be exploited for climb.

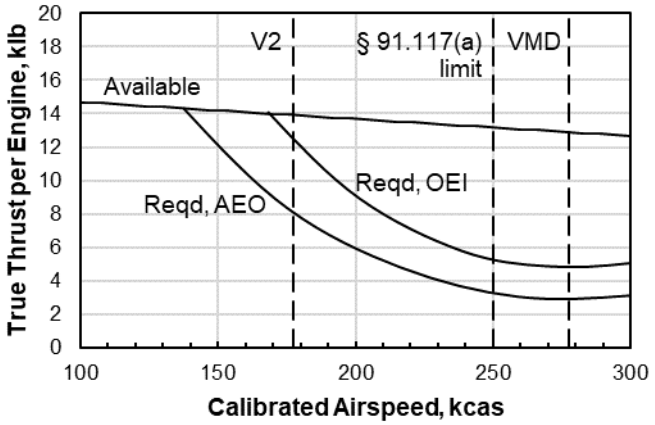

Figure 5. Thrust demand of the STCA for level steady flight.

Further, and in general, higher climbout speeds are preferred for most supersonic aircraft. The preference for high airspeed at low altitude can be shown for the STCA by constructing its thrust demand curves. These are shown in Figure 5 for level and steady flight at maximum weight at an altitude of 2000 feet. Noted in the figure is the takeoff safety speed (V_2), determined by a one-engine inoperative, balanced field calculation following the guidance in [47], and the 250kcas speed limit in the U.S. [48] and in many other countries. The STCA's minimum drag speed is nearly 280kcas. Speeds below this are in the so-called region of reversed command, where to fly more slowly requires more thrust to overcome increasing lift-dependent drag. This is in contrast to a similarly-sized subsonic airplane with takeoff flap deflections in these conditions, which may have a minimum drag speed of perhaps only 200kcas. Flying safely in this region requires adequate thrust margins, shown in the figure as the difference between available thrust and required thrust with all engines operating and with one engine inoperative. Supersonic transports are likely to have thin wings with low aspect ratios and simple flap systems. They are likely to require high takeoff speeds before sufficient lift is generated to lift off, and even higher airspeeds to climb with

significant thrust margin. In contrast with most subsonic transports, in-air acceleration segments to high airspeeds are preferred for supersonic transports. In operational practice, it was common for the Concorde to accelerate and to reach 250kcas by 400ft above field elevation [49], and similar in-air accelerations were planned for the proposed High-Speed Civil Transport [36, 45].

But for noise certification, in-air acceleration segments require attention. Unless permission is granted to operate otherwise, Section 3.6.2(d)(1) of [32] states that the climbout airspeed should be attained "as soon as practicable after liftoff" and it must be stabilized and maintained between V_2+10 knots and V_2+20 knots thereafter. But seemingly, as a result of the aerodynamic characteristics noted above, an excellent case could be made by supersonic airplane applicants to permit a departure from the speed requirement and accelerate to an airspeed higher than V_2+20 knots. And as already noted above, it is possible for the requirements of [32] to be waived if they are in conflict with an approved VNRS.

Thus, an acceleration segment shortly after takeoff would seem to be in order. In this study, the range of stabilized climbout airspeeds investigated for the STCA range from V_2+35 knots to V_2+55 knots, with the justification that higher airspeeds may be required to ensure adequate thrust margin and climb performance. High-lift devices are not retracted until the acceleration segment is completed. In operational practice, nearby aircraft may simply need to give more room to supersonic transports. This is already common today, where greater spacing intervals are given to large aircraft due to their wake turbulence.

IV. Noise prediction method

Another prerequisite for computing certification noise of the vehicle is an acoustic model. In general, aircraft system noise prediction tools fall into one of two categories. Both categories are discussed here, since (as will be shown later in this section) features from both are used in this study to determine noise along the lateral sideline.

The first category of tools rely on so-called noise-power-distance (NPD) data as the basis for computing noise on the ground. This approach was originally proposed by SAE [50], revised [51], and most recently documented by ICAO [52]. Original equipment manufacturers of civil aircraft supply NPD data for their products so that their noise impact may be modeled. Manufacturers measure NPD data directly, scale or infer them from other NPD data, or predict them from first principles using computational tools. System noise codes based on NPD input data are said to be "ICAO Doc. 9911-compliant" in accordance with [52]. Examples are the Aviation Environmental Design Tool (AEDT) [53] and others [54-57]. These tools, in a sense, start with the answer, because rudimentary noise characteristics for each airplane are given as tabular lookup data.

Other noise prediction codes, however, are less empirical and are based more on physics. They are more reliant on first principles, where lossless free-field spectra in the vicinity of an airplane are predicted and then propagated in a straight line to a receiver. Examples are NASA's Aircraft Noise Prediction Program (ANOPP) [58] and others [59-62]. The distinction between the two categories can blur, however, since codes like ANOPP can be coaxed into generating NPD data for use in Doc. 9911-compliant tools.

In this study, all noise predictions are made using ANOPP. But for the special case of noise along the lateral sideline (see Figure 4), a novel approach is used and a special adjustment is applied to the results using a feature borrowed from Doc. 9911. The method is discussed later in this section.

Predictive methods within ANOPP are selected to represent the noise sources of a supersonic business jet. It should be noted that applying empirical methods that were developed largely for conventional subsonic transports (powered by high bypass ratio, separate-flow turbofans) to a supersonic delta-wing airplane (equipped with low bypass ratio engines with supersonic inlets, long-duct mixers, and more complex nozzles) has a high uncertainty. Sensitivities to uncertainty are assessed in the previous study [4].

A. Source noise modeling

Jet noise is predicted using an empirical method developed by the Society of Automotive Engineers [63]. For simple, single-stream, round nozzles operating on the cusp of choke, the SAE method is preferred over other available methods based on comparisons of predicted levels to scale model and flight test data [64, 65]. Since jet noise is typically the dominant source in supersonic applications, it is the subject of recent studies at NASA [66-69].

Broadband fan noise is predicted using an empirical method developed by General Electric [70], and discrete fan interaction tones are predicted using a similar method [71] (both of these methods are more recent calibrations of ANOPP's original fan noise method). For predicting noise of high-speed, high-pressure-ratio, single-stage fans that might be used in a supersonic application, these methods are preferred based on comparisons made to data collected by NASA: the General Electric High Speed Fan [72], the Honeywell Quiet High Speed Fan [73], and a two-stage fan

designed and built by Pratt & Whitney as part of the NASA-led High Speed Research Program. Fan treatment suppression is estimated using a method developed by General Electric [74].

Engine core noise is predicted by a method developed by Emmerling [75]. Engine state data computed by NPSS are fed into ANOPP as functions of flight speed, altitude, and engine power setting.

Landing gear, flap, slat and trailing edge airframe sources are predicted using a recalibrated version of the empirical Fink method [76]. The recalibrated model is based on noise measurements of a supersonic delta-wing transport [77] and is documented in [78]. The predicted levels are adjusted using geometric inputs to represent airframe noise levels of a notional supersonic business jet.

With engines mounted above the vehicle, noise shielding effects must be considered. Shielding (also referred to as barrier attenuation or insertion loss) is an acoustic diffraction phenomenon where sound waves are attenuated when propagated past an impermeable barrier placed between the noise source and an observer. In this study, a simple empirical diffraction model based on optical diffraction theory is used. The model was originally proposed by Maekawa [79] and is reproduced in many foundational acoustic textbooks. Shielding is particularly efficient when the observer is located in the "shadow region" where the noise source is obscured. The delta wing (see Figure 1) provides excellent shielding of forward-radiated fan inlet noise. All other sources are not shielded. Jet noise is a distributed source generated downstream throughout the axial exhaust plume. Core noise is predominantly aft-radiating and is assumed to radiate through the exhaust. Fan exit noise also escapes through the nozzle but it is attenuated by treatment in the bypass duct.

B. Noise propagation and special considerations for lateral receivers and supersonic transports

Noise levels of all components are predicted as lossless, one-third octave band spectra and are summed in the vicinity of the airplane. The noise sources are analytically flown along the trajectories to be described in the following section and are propagated to noise monitors located on the ground. The source levels are computed at half-second intervals using engine state data for the flight condition and engine state given by the reference profile. This is particularly important in modeling noise during procedures where the engine state is dynamically varying, such as during the proposed PLR procedure. Noise propagation effects include spherical spreading, Doppler shift and convective amplification, atmospheric absorption [80], and ground reflections [81, 82] based on data for grass-covered ground [83].

Ground reflections and lateral attenuation due to refraction and scattering are two effects of acoustic propagation that can strongly influence noise received by a lateral observer. Software that predicts community aviation noise in the manner of ANOPP are reliant on classical, physics-based ground reflection models to predict noise at receivers. However, empirical lateral attenuation models often include the influence of ground reflections implicitly, and so a double-bookkeeping error can exist if one is used together with a classical reflection model.

The classical, physics-based reflection model in ANOPP [81, 82] is somewhat idealized. It does not capture the effects of atmospheric refraction and scattering of sound signals due to wind and variable meteorological conditions, variable ground characteristics, and aircraft configuration. Lateral attenuation is generally underestimated by theoretical methods such as these, particularly for elevation angles above grazing incidence [84, 85]. So modeling noise at laterally-displaced receivers using a classical reflection model alone neglects some of the "free" lateral attenuation provided by nature.

This shortcoming invites the use of an empirical lateral attenuation model when predicting lateral noise. The Society of Automotive Engineers, in Aerospace Information Report (AIR) 5662 [40], provides an approximate model of lateral attenuation for flat, soft ground and average meteorological conditions. They define lateral attenuation as the attenuation of sound from an airplane to a laterally displaced receiver that is not attributed either to atmospheric absorption or to spherical spreading. In developing the model, researchers measured noise from a variety of aircraft using centerline and lateral microphone pairs mounted on 1.2 m poles. For each flyover event, the maximum level measured directly under the flight path was subtracted from the level measured at the companion lateral location. Spreading and absorption components were removed, with the remainder deemed lateral attenuation. The model is derived from a database of these differences. The empirical model is developed from curve fits of A-weighted sound exposure level and effective perceived noise level metrics, and it is claimed to represent several other noise metrics well. In Doc 9911-compliant tools, lateral attenuation is one of several effects that are subtracted from NPD data, regardless of the choice of NPD metric.

Lateral correction methods, like AIR 5662, are intended to work with Doc 9911-compliant tools. Reflection effects of 1.2m pole-mounted microphones above a flat, soft ground surface are implicitly captured in NPD data, and as such, Doc. 9911-compliant tools are not afflicted with a bookkeeping issue. AIR 5662 is compatible with this arrangement by way of its measurement strategy. But, as already noted, the accounting is incompatible with system noise codes

based on first principles, like ANOPP. Thus, bookkeeping issues can put modelers in a quandary. Reflections, refraction, and scattering are first-order influences on received noise, and methods to account for them are needed. But accounting for these effects may not always be consistent. A more thorough discussion of these issues as well as a bookkeeping correction proposal can be found in [86].

To date, subsonic airplane analysts using codes in the style of ANOPP have not been overly concerned with the lateral bookkeeping issue. Conventional subsonic airplanes do not (yet) manipulate engine power at low altitudes. So, when predicting noise at laterally-displaced receivers, researchers typically make noise calculations once the aircraft is aloft. When the airplane is sufficiently high, the effects of refraction and scattering become small (see, e.g., [40]), rendering the bookkeeping issue moot. The lateral noise prediction is usually made where the point of closest approach of the airplane subtends an elevation angle of 30 to 40 degrees with the horizon. At that point, most of the refraction and scattering effects have faded and the lateral noise level reaches its peak. Thus for most conventional subsonic airplanes, the use of a classical reflection model alone is sufficient.

But the bookkeeping issue can become a matter of some importance to makers of proposed early market entrant civil supersonic transports. This is especially true of manufacturers who do not have access to relevant data and who may rely on first-principles codes, like ANOPP. Unlike subsonic transports where takeoff engine power is maintained throughout the lateral noise measurement period, manufacturers of new supersonic transports are likely to use a PLR procedure. The timing and the amount of thrust reduction are variables left to the type certificate applicant. It would be unfortunate if an applicant developed a PLR procedure only to discover that maximum lateral noise occurred before the programmed thrust reduction took place while their airplane was still near the ground! The purpose of the PLR procedure would be lost if lateral attenuation effects were overestimated. Thus, accurate modeling of lateral effects is particularly important for supersonic transports.

C. Lateral noise measurement and speculation on future VNRS field testing

In light of the noise bookkeeping issues discussed above, and because the STCA performs a PLR procedure (the design of which is yet to be defined), a special lateral noise calculation method is required. The noise metric regulated by [32] for certification of large, transport-category and jet-powered airplanes is the effective perceived noise level (EPNL, with units of EPNdB). The EPNL is a duration-dependent, single-event noise metric determined from a set of instantaneous noise levels versus time. The instantaneous noise metric is the tone-corrected perceived noise level (PNLT, with units of TPNdB). As the airplane approaches and then recedes, PNLTs are defined at half-second intervals. From these, an EPNL is computed. Only PNLTs within 10TPNdB of the maximum level are used. The lateral EPNL is defined as the maximum level along the entire lateral sideline (see Figure 4).

With a Doc. 9911-compliant tool such as AEDT, computing any number of EPNLs along a lateral sideline is straightforward. But for reasons discussed previously, this is not so for a tool based more on physics such as ANOPP. With a code like ANOPP, blithely assuming that the lateral EPNL reaches its maximum once the airplane is aloft is likely to be insufficient for an applicant proposing a PLR procedure. So instead of the usual practice of making a single lateral EPNL calculation at a point when the airplane reaches an elevation angle of 30 to 40 degrees, multiple EPNL calculations should be made all along the lateral sideline. Every calculation made will have a unique set of instantaneous noise levels and a unique time interval (i.e., the so-called “10dB-down” period).

Since the lateral EPNL is defined to be the maximum level along the sideline, EPNLs *before and during* the PLR procedure must be calculated to ensure that the highest EPNL *after* the PLR procedure is the maximum. If this condition goes unmet, then the purpose of a PLR procedure is rendered moot and pointless. Thus, the lateral array of receivers should be long enough to capture EPNL behavior before, during and after the PLR procedure. In this study, the first EPNL in the array is evaluated at a point where the airplane is still on the runway, while the last EPNL is evaluated at a point after the airplane has reached an altitude high enough that noise has begun to diminish.

Within many of the lateral 10dB-down periods, thrust may be lapsing at a rate determined by the PLR procedure, and airspeed may not yet have stabilized. And at low elevation angles, various meteorological lateral ground effects are likely to complicate noise propagation as discussed above. Thus with so many variables, making a lateral EPNL calculation during a PLR procedure is analytically thorny. It will also be challenging to accommodate an applicant proposing one in the field. In the vernacular of some certifying authorities, complexities or instabilities within the 10dB-down period are sometimes called “intrusions.” A PLR procedure resulting in multiple intrusions may make equivalent testing challenging. Equivalent testing procedures are simplifications typically used in noise certification tests. They allow an applicant to avoid taking off and landing repeatedly for every noise measurement. Equivalent procedures are designed to simplify the reference profile while having no impact on noise at monitoring stations. Without actually taking off, a pilot will fly a course low over the ground that intercepts the reference climb path well before the noise monitoring station. After the interception point, the airplane follows the reference climb path. But

with no flight test experience and without data, it is unclear how equivalent procedures could be designed to accommodate a PLR VNRS. This is also true for a programmed flap retraction VNRS, though perhaps to a lesser extent. The first field measurements of these VNRS procedures promise to be groundbreaking.

D. Lateral noise prediction methods

Several methods of evaluating lateral noise are possible using either a system noise prediction tool such as ANOPP, or with a Doc. 9911-compliant tool such as AEDT. For the special case of an airplane having a VNRS where engine power is manipulated at low altitude, no method is flawless. Five options are discussed below.

Option 1: System noise prediction tool with traditional lateral receivers

ANOPP and other system noise prediction tools are programmed with classical ground reflection calculators. These tools can be used to evaluate noise at a receiver placed on the lateral sideline. Traditionally, and as already noted above, this is acceptable as long as the receiver is located across from the point where the airplane has reached perhaps 1000 feet above field elevation (where refraction and scattering effects are small) and as long as engine power remains constant. But when a PLR procedure is used to manipulate engine power shortly after liftoff, lateral noise should be evaluated earlier in the takeoff when the airplane is at lower altitude. Here, the effects of refraction and scattering are not small and should no longer be ignored. This shortcoming invites the use of an empirical lateral attenuation method (e.g., [40-43]) that does capture these effects. But, as already noted, they are incompatible with classical reflection models. Thus, this option is not acceptable for the present problem.

Option 2: Doc. 9911-compliant tool with centerline receivers

As noted earlier, ANOPP can be coaxed into predicting NPD data. These can be used subsequently in a tool such as AEDT to evaluate lateral noise in the manner of Doc. 9911. This is the traditional way to evaluate lateral noise in Doc. 9911-compliant tools. It captures properly the behavior of lateral noise attenuation using NPD data evaluated for centerline receivers. Empirical lateral attenuation methods such as AIR 5662 are compatible with NPD data by design. Development of NPD data for the STCA for use in ICAO studies is the subject of [16].

However, using NPD data to compute lateral noise becomes quite thorny for complex takeoff profiles using one or more VNRS procedure while at low elevation angles. With PLR and automatic flap retraction procedures in use, throttle setting, airspeed, flap deflections, distance, climb angle, and lateral attenuation effects change together dynamically, causing multiple intrusions within the 10-dB down period. Assembling an accurate PNLT vs. time noise history using NPD data would be difficult and prone to error, since traditionally, NPD data simply are not functions of enough independent variables.

Work, however, is underway [87] that may result in adding additional independent variables to traditional NPD data. With such "enhanced" NPD data, it should be possible to break the takeoff profile into enough small discrete segments so that VNRS procedures at low altitudes are properly modeled. If the recommendations of the study are accepted, the logic to use the enhanced NPD data would need to be coded into AEDT. For now at least, this option is not acceptable for the present problem.

Additionally, an ANOPP noise model may in some cases depend upon the azimuthal emission angle (i.e., in the roll direction of the airplane). Since NPD data are evaluated on the extended runway centerline, and since noise is predicted in the nadir direction only, NPD results are insensitive to this dependency. As is the case with all Doc. 9911-compliant tools, NPD data are reliant upon an empirical geometric effects and engine installation term in AIR 5662 to account for the directional effects associated with configuration and engine placement. This is true for NPD data in general, whether they are computed by ANOPP or by other means. The term accounts for airplane surfaces influencing shielding, reflection, and refraction of sound in the vicinity of the airplane, as well as for jet-by-jet shielding of jet engine exhausts. The installation term is a function of the depression angle (equal to the elevation angle when the airplane bank angle is zero). Use of this term is thus in conflict with any directivity effects already incorporated in the source noise models of ANOPP. Modelers using ANOPP to compute NPD data must be satisfied with this accounting, at least with the present NPD format.

Option 3: Hybrid approach using a system noise prediction tool with centerline receivers

A hybrid approach is inspired by a combination of the first two methods above. Like the first option, this approach uses a system noise prediction code such as ANOPP. But rather than arrange receivers along the lateral sideline, receivers are arranged on the extended runway centerline, such that the airplane passes above them directly overhead. The code is executed with ground reflection calculations enabled. The resulting one-third octave band sound pressure levels received at each centerline location are used to *infer* levels at companion lateral sideline receivers at the same

distance from brake release. This is accomplished by adjusting each received noise spectrum for spherical spreading and for absorption differences using simple geometry, i.e., the airplane height above the centerline relative to the lateral slant distance. This adjustment requires an assumption of straight-ray propagation in the manner of ANOPP. These adjustments are not a feature of ANOPP and so they must be made on a post hoc basis using a custom tool. Once the inferred sound pressure levels on the sideline are known, a correction for lateral attenuation can be made. This is done by applying the lateral attenuation correction specified by AIR 5662 to each sound pressure level in the spectrum. Using these adjusted spectra, new sets of revised PNLTs can be computed, and from these, lateral EPNLs can be calculated. Although AIR 5662 is not expressly stated to be a single-frequency model, its apparent versatility suggested in [40] and discussed in [86] implies that it could be used as such. Additionally, as is the case with the second option above, modelers must be satisfied with the installation term in AIR 5662 to account for azimuth angle influences.

Thus, this option avoids the ground effects bookkeeping dilemma by extending the philosophy of Doc. 9911 to system noise prediction codes. This seemingly-attractive solution fails in some cases, however. When an airplane passes a centerline receiver directly overhead at a low altitude, the polar emission angle (i.e., in the yaw direction of the airplane) transitions very rapidly from the forward quadrant to the aft quadrant. But for a lateral receiver, the transition is more gradual since it is at a greater distance. This results in a polar angle mismatch in the time histories at lateral positions relative to centerline positions. So if centerline noise is to serve as a surrogate for lateral noise, an error is introduced for any noise source having a dependency on polar angle. Jet noise is strongly dependent on polar angle, and it dominates the STCA's noise signature during takeoff. And though the error diminishes once the airplane is sufficiently high, VNRS procedures are anticipated to occur at low altitudes. Thus, this option is not acceptable for the present problem.

Option 4: System noise prediction tool with lateral receivers and an accounting correction

An accounting method has been proposed [86] that reconciles the bookkeeping conflict between the Chien-Soroka ground reflection model and the AIR 5662 lateral attenuation model. It allows system noise prediction tools that are reliant on straight-line spectral propagation to compute lateral noise levels that are more agreeable with measurements made in the field. A simple field correction adjustment term is derived that ensures the behavior expected from the lateral attenuation model. Applying the term to received spectra forces consistency between reflection and lateral attenuation models on an overall, frequency-integrated basis.

This method is not coded into ANOPP and thus it would need to be applied on a post hoc basis using information contained in ANOPP's output. Further, for receivers located above a reacting surface, the field correction term is necessarily a function of frequency. Thus, applying it reshapes received spectra in perhaps an unrealistic manner. The spectral distortion impacts integrated metrics such as PNL, PNLT, and EPNL. The distortion is greatest at low elevation angles, which is precisely the region of interest of a low-altitude PLR procedure. Thus, this option is difficult to justify when a VNRS is used at a low altitude.

Option 5: System noise prediction tool with centerline receivers and "pseudo altitudes"

This is the method selected for the present study. Lateral EPNLs are computed using ANOPP (albeit unconventionally), with guidance taken from Doc. 9911 and AIR 5662. Like options two and three above, noise is evaluated for observers placed along the extended runway centerline, such that the airplane passes above them directly overhead. Ground reflection calculations are enabled. However, the takeoff reference profile is not provided to ANOPP in the usual manner. Instead of using a takeoff profile based on the true airplane altitude, a "pseudo altitude" profile is used. The pseudo altitude is simply the lateral slant distance between the airplane and the lateral sideline, i.e., $\sqrt{h^2 + s^2}$, where h is the true altitude above field elevation and s is the 1476ft displaced lateral sideline distance (see Figure 4). Pseudo altitude and true altitude are plotted in Figure 6 for the takeoff reference profile used in [4].

When the pseudo altitude is substituted for the true altitude, noise levels on the centerline can be evaluated straightforwardly by a system noise prediction tool like ANOPP. Noise at any centerline location is thus representative of noise on the lateral sideline at the same distance from brake release. Spherical spreading and atmospheric absorption effects for a lateral position are captured correctly since the slant distance is used in place of true altitude. Afterwards, EPNLs can be adjusted safely for lateral attenuation (without a ground effects bookkeeping conflict) using AIR 5662, making the lateral EPNL agreeable to measurements made in the field.

The lateral and flyover EPNLs share the same true takeoff profile. The flyover EPNL is evaluated ordinarily, using the takeoff profile with true altitudes. Since the flyover EPNL uses true altitude, it must be calculated in a simulation separate from the lateral simulation.

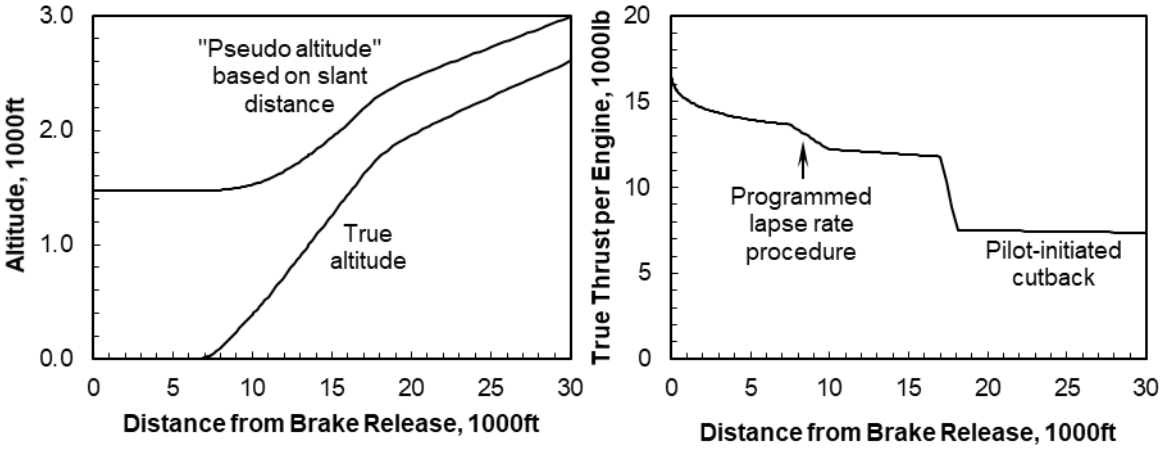

Figure 6. "Pseudo altitude" defined for a sample takeoff reference profile.

1. Errors associated with the method

Three modeling errors are identified if pseudo altitudes are used in place of true altitudes. But the errors are considered to be minor, at least for the present STCA problem. The errors can be illustrated best by writing the equation for straight-ray sound propagation from a source at a pseudo altitude H to a pole-mounted receiver at a height h above the ground. The equation below accounts for propagation effects modeled in the manner of NASA's ANOPP, with an additional term taken from AIR 5662.

$$L_{rec} = L_{src} - 20\log_{10}[r_D/r_{ref}] - \alpha r_D + 10\log_{10}[(\rho_h c_h)/(\rho_H c_H)] + 10\log_{10}G - \Lambda$$

L_{src} is the source level at a reference radius r_{ref} taken in the vicinity of the airplane. It consists of sound pressure levels measured in decibels relative to 20μPa. They are dependent on frequency, emission angles, flight condition, and engine-airplane state. L_{rec} is the received level on the ground track of the airplane (i.e., on the extended runway centerline), following modification by several propagation effects represented by terms on the right hand side of the equation. For an arbitrary point on the takeoff profile, r_D is the direct path length from the centerline receiver to an airplane flying at the pseudo altitude H. In the special case when the airplane is directly over the receiver, $r_D = H - h$. The term α is the atmospheric absorption coefficient (representing the total of several varieties of atmospheric dissipation) with units dB per unit length. The effects of spherical spreading and atmospheric absorption are accounted for by the second and third terms on the right hand side of the equation. The remaining terms are identified below. So even though L_{rec} is evaluated on the centerline, it is representative of noise at a lateral receiver whenever pseudo altitudes are used, at least insofar as spreading and absorption are concerned.

The first modeling error when pseudo altitudes are used is related to ray propagation phenomena arising whenever a layered, absorbing atmosphere is defined. In ANOPP and in other tools, an average value of α is computed whenever a nonhomogeneous atmosphere is defined. Also, characteristic impedance is the product of local air density ρ and the speed of sound c. In ANOPP, an impedance correction is applied during propagation so that acoustic power is conserved at both ends of a propagating ray represented by a conical tube. The fourth term on the right hand side accounts for this effect (where ρ and c are evaluated at h and H). Errors in these terms are introduced if the pseudo altitude is used in place of the true altitude. These errors are greatest for a situation where the airplane is still on the ground (i.e., when the true altitude is zero and the pseudo altitude is 1476ft, as in Figure 6). Using a standard atmospheric model, the difference in absorption and impedance effects between sea level and 1476ft leads to an error of just 0.2dB. The magnitude of the error decreases afterwards as the airplane lifts off and climbs. The error could be dealt with by recoding or by post-processing. In this study, the error is simply accepted.

The second modeling error when using pseudo altitudes involves the field correction term G that accounts for ground reflections. The Chien-Soroka reflection method [81, 82] is coded into ANOPP and other tools. A rote recitation of the method as coded into ANOPP is presented in [88] in recipe format. The major independent variable in the method is the path length difference (i.e., the difference in length between the direct ray from the source to the receiver and the length of the reflected ray). In an arbitrary geometry, variable airplane positions result in variable elevation angles and path length differences. So whenever pseudo altitude is used in place of true altitude, G takes on a spectral shape that is different than its "true" shape and an error is introduced. The magnitude of this error must be

small if this method is to be viable. Since this method uses centerline receivers as substitutes for lateral receivers, consider first the special geometric case when a source is located directly over a receiver (i.e., the zenith geometry, when the elevation angle is 90 degrees). Here, the path length difference is reduced to a simple constant. It is equal to twice the receiver height above the ground, and it never changes regardless of the source height. The complex ground wave function (a term that accounts for the difference between a plane wave reflection and a spherical wave reflection) for this arrangement is essentially zero. So whenever the elevation angle is 90 degrees, G remains constant regardless of whether true altitude or the larger pseudo altitude is used. This is good news for the proposed method, but whenever elevation angle is less than 90 degrees, the error becomes nonzero. The error is difficult to quantify in any general sense since several variables are involved. But it is quite stable on an overall (i.e., frequency-integrated) basis. That is to say, the ground peaks and nulls are positive and negative in approximately equal measures (see, e.g., Figure 2 in [86]). Therefore on an integrated basis, the error does not grow beyond 0.1dB until the elevation angle falls below about 20 degrees (and by that point, noise typically has fallen outside of the 10dB-down region of interest). The frequencies at which the peaks and nulls occur, however, shift as elevation angle changes. So a source having significant tone content may be expected to incur a greater error than a broadband source if its tones are modified by ground nulls as the profile is traversed. But in the case of the STCA during takeoff, the noise signature is dominated by broadband jet mixing noise. This leads to an EPNL error on the order of just 0.2 EPNdB. The error could be dealt with by recoding (i.e., by forcing the phase angle to remain equal to the value calculated in the zenith geometry). In this study, the error is simply accepted.

The third error is the method's insensitivity to any azimuthal radiation effects that may already be built into an ANOPP model. This weakness has already been identified in options two and three discussed above. The AIR 5662 lateral effects term Λ includes an installation correction to capture azimuthal variation. Elevation angle is its major independent variable. The intrinsic ANOPP methods used for the STCA during takeoff are weak functions of azimuth angle and elevation angle. More specifically, the wing shielding analysis used [79] introduces an azimuthal dependency for forward-radiated fan noise, but it is so effectively shielded by the wing that it makes little difference. The jet noise model used [63] is not a function of azimuth angle, and since angle of attack is generally small, it is also not a strong function of elevation angle. And though airframe noise is dependent on azimuth angle, it is not predicted to be a significant contributor to noise during takeoff. Thus in the case of the STCA, it seems wholly appropriate to address the jet-by-jet and engine mounting effects of installation on lateral noise in a post hoc manner within Λ as suggested in [40]. Empirically-derived estimates for these effects are given in [40] for the following three popular engine installations: airplanes with underwing-mounted engines, airplanes with rear-fuselage-mounted engines, and for propeller-driven airplanes. The fuselage-mounted option is used in this study.

2. Using the method to inform a VNRS design

The proposed method reconciles the ground effects bookkeeping conflict between physics-based system noise prediction tools and Doc. 9911-compliant tools. It is an appealing choice for evaluating a takeoff VNRS taking place at low altitude. With PLR and automatic flap retraction procedures in use, throttle setting, airspeed, flap deflections, distance, climb angle, and lateral attenuation effects change together dynamically, causing multiple intrusions within the 10-dB down period. This method allows an accurate PNLT vs. time noise history to be captured accurately for arbitrary lateral receivers. When the STCA is at low elevation angles – and is perhaps performing a PLR procedure – computing lateral noise in this manner allows proper bookkeeping of effects.

It also has the ability to troubleshoot the design of a PLR procedure. If lateral noise is evaluated all along the 1476-foot sideline, then EPNLs of the airplane before, during, and after the PLR procedure can be determined accurately and can be compared. If a lateral EPNL evaluated at a point before the PLR procedure is the maximum of all of the lateral EPNLs, then the design of the procedure is invalid (i.e., the thrust reduction is either too great or it occurs too late to be effective).

A PLR procedure can be designed that minimizes either lateral noise or flyover noise (or both, via cumulative noise), depending on noise margin requirements. Of course for a manufacturer with an actual product, a design having sufficient margins must be in hand before field testing begins. In the absence of measured data, and with untested procedures, new technologies, and with an unconventional configuration involved, margins should be greater than those used for conventional subsonic airplanes. In pre-test modeling, manufacturers should not overestimate the benefits of lateral attenuation. It would be unfortunate if so much trust was placed in a lateral attenuation model that it resulted in a PLR procedure that did not work as expected. As evidence, one need look no further than the scatter of attenuation measurements shown in [40].

V. Takeoff reference profiles

A. Statement of problem

A takeoff reference profile that makes optimal use of the combined PLR and flap retraction procedures is desired. Minimum lateral and flyover certification noise levels are sought. The design of the VNRS procedure is important since the takeoff profile and engine power settings significantly influence noise during takeoff. As in previous NASA STCA studies [3-5], all takeoff profiles are computed using a forward-differencing trajectory solver [30]. Calculations assume a sea level runway and use standard acoustic day conditions.

The lateral EPNL is influenced directly by the VNRS, while the flyover EPNL is influenced by the prior events of the VNRS. And so the optimum VNRS must consider both lateral and flyover EPNLs. Thus, a composite objective consisting of the cumulative EPNL (i.e., the algebraic sum of the three certification EPNLs) is optimized. The approach EPNL remains constant (as determined in [4]), and it does not contribute variability to the objective.

The VNRS design variables to be optimized are:

1. Magnitude of thrust lapse
2. Beginning of thrust lapse and in-air acceleration segment
3. End of thrust lapse and in-air acceleration segment
4. Stabilized airspeed
5. Flap retraction altitude

In this study, the takeoff VNRS procedure is confined to events following clearance of the 35-foot runway obstacle. All performance assumptions made in [4] such as decision speed, rotation speed, and takeoff safety speed remain unchanged. Normal takeoff field distance with all engines operating and the critical (balanced) field distance with one engine inoperative are also unchanged. The takeoff flap deflection study is described in [4]. Initial leading- and trailing-edge flap deflections determined by the study are unchanged (though unlike [4], flaps are retracted afterwards here via the VNRS). At brake release, leading- and trailing-edge flaps are deflected to angles of 6deg. and 10deg, respectively.

In this study, the VNRS procedures are not overly complex. They are designed with an eye toward eventual implementation in a product, such that the airplane behaves like most others within the terminal airspace. And simpler procedures stand a greater chance of having equivalent testing procedures represent them. Engine throttle manipulations are simple and climb rate requirements of airworthiness regulations [47] are met. Thrust lapses linearly with time, and once thrust has decreased, it does not increase (within the terminal airspace, at least). Calibrated airspeed is held constant after it has stabilized to the climbout speed required by the problem. A more mathematically ambitious optimization is being investigated by Voet [11, 89], building upon his work reported in [90]. His plan is to use optimal control with automatic differentiation to design an engine for the STCA that is optimized for noise and emissions.

Note that the more familiar pilot-initiated cutback is not considered in this paper to be part of the VNRS procedure. Engine thrust may be cut back to a minimum level defined by [32] to reduce flyover EPNL. Properly optimized, the pilot-initiated cutback should result in a flyover EPNL engine power incursion (i.e., having portions of post-PLR thrust and cutback thrust within its 10dB-down period). Applicants normally exploit this provision to reduce the flyover EPNL (it is discussed thoroughly in [14]). Since the cutback takes place after the VNRS procedure (but yet is influenced by it), its timing can be optimized independently after the VNRS is optimized, and so it need not complicate the main optimization.

B. Factorial design of experiments

A parametric driver is constructed that performs a trajectory calculation and a corresponding noise analysis for any given set of design variables. With only five VNRS design variables (excluding the cutback timing), and since the computational cost of each sample is not unreasonable, there is little reason to apply an optimizer to the driver. This is particularly true if the objective is noisy or if the design space turns out to be riddled with local optima (though it is difficult to know this at the outset). Instead, it is straightforward enough to "paint the design space" using a factorial design of experiments. This type of grid-based optimization is an "exhaustive search." The cost of this brute-force strategy is higher than a search aided by an optimizer. But if each objective sample runs reasonably fast, it is attractive since finding the global optimum is virtually ensured (provided the grid intervals are sufficiently fine). The optimal VNRS design is selected simply by inspection. The danger of an optimizer becoming "stuck" on a local optimum is thus avoided. Though if necessary, an optimizer could be applied using the best result of the factorial

experiment as a starting point. The design variables and their limits are shown in Table 4. The variables are cast into terms recognizable to the trajectory solver [30]. With this factorial and with the grid intervals selected, 6000 samples require evaluation.

Table 4. VNRS design variables and ranges investigated.

Design variable	Minimum	Maximum
Programmed thrust lapse, %	10	34
Programmed thrust lapse beginning altitude, ft	35	155
Programmed thrust lapse rate, %/s	1.0	4.0
Stabilized airspeed (increment above V_2, kcas)	35	55
Flap retraction altitude (increment above stabilized speed altitude, ft)	0	600

Some combinations of these design variables may be nonsensical. For example, some combinations of the PLR procedure timing and its rate of thrust decay may lead to cases that encroach upon the pilot-initiated thrust cutback. Nonetheless they are included in order to have an orthogonal design space. Nonsensical designs are simply ignored when selecting the optimum design.

VI. Results and discussion

The minimum cumulative noise solution is found to correspond to a VNRS having a 30 percent thrust lapse that begins immediately after clearing the runway obstacle. During the PLR procedure, thrust lapses at a rate of 2 percent per second. Stabilized airspeed is 55kcas above V_2, and high lift devices are retracted just as the stabilized airspeed is reached. This solution is shown in Figure 7. Altitude above field elevation, calibrated airspeed, true thrust per engine, and lateral EPNL are plotted against distance from brake release. The Annex 16 lateral EPNL is the largest of the EPNLs along the sideline (88.8 EPNdB), as indicated in the figure.

Lateral EPNLs at locations less than 5000ft from brake release are not computed. Early in the ground roll, forward speed is low and as a result, the duration component of the EPNL metric increases. In the figure, levels can be seen to increase towards the point of brake release. The EPNL noise metric is ill-defined in static or in low-speed situations. To compute the metric near the point of brake release would be novel and perhaps unorthodox in a certification scenario. Additional clarity from regulating authorities on this issue may be needed.

The 30 percent programmed thrust lapse for minimum cumulative noise is much larger than the unoptimized 10 percent lapse assumed in the previous study (Ref. [4], also shown in Figure 7). For comparison, a 30 percent thrust lapse is slightly more than what is being considered by Boom Technology for their Mach 1.7 Overture transport [91]. There are several risks involved with large programmed thrust lapses. They are discussed below.

Among the most demanding requirements for the STCA's VNRS are the minimum climb gradients required by sections 111 and 121 of [47] for trijets with one engine inoperative. Even so, once the 35-foot runway obstacle is cleared and the PLR procedure begins, the STCA appears able to tolerate quite large thrust lapses before the climb gradient constraints become active. This may not be the case for any airplane, however. The STCA has narrowly-spaced engines mounted on its rear fuselage, and thus its engine-out yaw drag increment is low compared to transports having underwing-mounted engines with wider spacing. Climb gradients for supersonic transports having more widely-spaced engine configurations may differ. But just because the STCA can tolerate such a large programmed thrust lapse does not mean its engine is oversized. High thrust is required during the ground run in order for the Part 25 [47] takeoff field distance to be 7000ft. Its derivative engine and its planned takeoff derating is discussed in more detail in [4].

A concern of having a large programmed thrust lapse occurring at low altitude during initial climb is the time required to increase thrust of the operating engines if one engine becomes inoperative. In such a situation, an automatic thrust control system might be used to increase thrust without need for crew intervention. Regulations governing automatic takeoff thrust control systems were defined under 14 CFR § 25.904 in 1987. For example, special conditions for automatic power increases have been granted to the Embraer 170/190 family [92] and to the Airbus A320 series [93], though not for PLR procedures. The time to spool the engines up to maximum power must be considered, and so the amount of programmed thrust lapse could be limited.

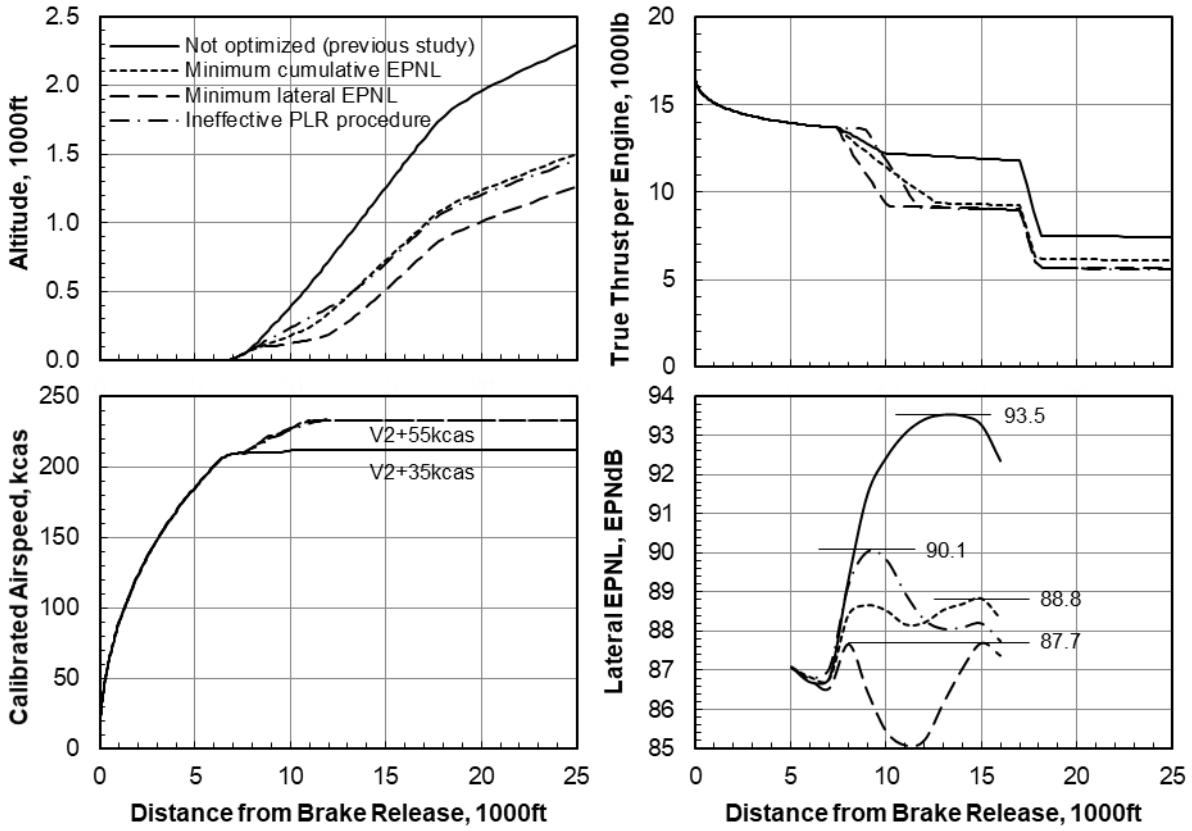

Figure 7. Takeoff profile solutions.

One possible approach to reducing engine spool up times is to not spool them down in the first place. It is possible for supersonic engines to have variable-geometry nozzle throats (in addition to variable nozzle exits). The likelihood of needing throat variability increases with cruise Mach number. For subsonic separate-flow turbofans having low fan pressure ratios, variable-area bypass nozzles are seen as one solution to the fan stall margin problem [94], and they have the added ability to control thrust [95]. In such an engine, thrust can potentially be reduced without sacrificing spool speed by opening the nozzle throat while reducing fuel flow. Engines might respond more quickly to throttle commands to increase thrust sharply at critical times. But the STCA's engine is a mixed-flow turbofan with a forcible lobed mixer. If this tactic is used in a mixed flow engine, flow rate remains high in the bypass duct while core pressure falls. In the STCA engine, the mixing solution results in high mixer port Mach numbers (particularly in the bypass port, which very quickly approaches choke). This problem could be lessened by selecting a different design extraction ratio, but with a loss of cycle efficiency. Further, reliance on actuated parts at relatively low altitudes introduces risk.

Accelerating to V_2+55kcas (the highest climbout airspeed investigated) is an attractive means to reduce noise. A climbout at higher speed results in less shear between the jet plume and ambient air, weaker turbulence, and less jet mixing noise. Higher airspeed also allows flaps to be retracted. This, in turn, results in a higher lift-to-drag ratio and a deeper pilot-initiated engine thrust cutback to the minimum climb gradients permitted by [32] (see Figure 7). Last, a higher speed climbout results in generally lower noise due to shorter event duration.

Lateral noise continues to fall in many cases where thrust is allowed to lapse beyond 30 percent. But cumulative noise is found to increase for these cases, since climb rate is poorer and airplane altitude at the flyover monitor is lower. For this reason, calculations for thrust lapses greater than 34 percent are not investigated. The minimum lateral EPNL solution found in this range is shown in Figure 7. It has two equal noise peaks; the first occurring before the PLR procedure, the other afterwards. This is similar to the behavior expected by Lockheed Martin Corp. in [96]. Note the first peak could be reduced theoretically by performing the ground roll at a reduced thrust, but it would come at the cost of longer takeoff field distance.

The minimum cumulative noise solution also has two noise peaks, though not precisely equal. Indeed, a solution with even lower cumulative noise should be possible if the requirement of monotonically reducing thrust once airborne is removed. If thrust is allowed to increase between the two lateral noise peaks, the airplane will have gained additional

altitude over the flyover monitor. Manipulating the throttle should lead to a lateral noise plateau rather than two peaks. This behavior can be seen in Voet's optimum [89] in which a "thrust bump" appears.

A solution having an ineffective PLR procedure is also shown in Figure 7. In this case, the thrust lapse is large and it occurs somewhat late. Thus, peak lateral noise occurs before the thrust lapse takes place, rendering the PLR procedure moot. Other details of the profile, however, are not much different than the optimum profile. This underscores the need for accurate modeling of lateral effects: they are necessary to eliminate ineffective VNRS designs like these.

Overall noise results are shown in Figure 8. In each plot, published noise type certificate data of subsonic aircraft are shown. Levels of over 11,000 Chapter 4 aircraft types are plotted against maximum takeoff gross weight. Chapter 3, Chapter 4, and Chapter 14 maximum limits for subsonic transports are also plotted in the figures. The "Supersonic Level 1" (SSL1) limit proposed by the FAA in 2020 [35] for three-engined supersonic transports (weighing up to 150,000lb and having a maximum cruise Mach number of 1.8) is also shown. EPNLs optimized for lowest cumulative noise are denoted by the solid symbols. The unoptimized solution using the takeoff reference profile from the previous study [4] is denoted by the open symbols. The STCA's approach reference profile is unchanged, and so the approach EPNL does not change relative to the previous study.

Previously, a relatively small programmed thrust lapse of just ten percent was assumed. But results of this study indicate that a much more aggressive PLR procedure can be used to reduce lateral noise. And when combined with an automatic flap retraction procedure and an acceleration segment, lateral noise can be reduced without necessarily increasing flyover noise. With this VNRS, cumulative noise of the STCA is predicted to be 271.9 EPNdB, or 5.2 EPNdB lower than the level predicted in the previous study [4]. This level is quiet enough to satisfy SSL1 requirements of 2020 [35] with 2.5 EPNdB of margin.

Since 2020, results of the CAEP supersonic exploratory study [97, 98] have become available. Though the study was intended to simply provide information to CAEP and not to prejudge the need to set noise stringencies for future supersonic transports, it did highlight the differences in noise between the notional supersonic transports analyzed (including the STCA) relative to the subsonic fleet. At this writing, the U.S. now supports [99] a proposal from industry [100] to limit noise of supersonic airplanes to the same Chapter 14 standards used today by subsonic airplanes. But even with the VNRS optimized in this study, the STCA is predicted to fall short of Chapter 14 standards by 1.0 EPNdB.

Additional noise reduction technologies could be used to reduce levels further to Chapter 14 limits. Nozzle chevrons, for example, can be an effective means of reducing jet noise by promoting earlier mixing of the exhaust stream with ambient air and causing a reduction in the jet's overall turbulent kinetic energy. But they also introduce a nozzle gross thrust penalty, which increases with the amount of chevron penetration into the exhaust stream. Nozzle chevrons are used in some contemporary subsonic applications, and they could be available for a near-term supersonic application. In the previous study [4], the cumulative noise benefit of adding chevrons was estimated to be 2.7 EPNdB, which could bring the STCA to within Chapter 14 limits. Chevrons, however, were predicted to cause range to decrease from 4243nmi to 4123nmi; a 2.8 percent penalty. Additional margin to guard against unexpected increases would likely be required for new supersonic transports.

VII. Summary

Manufacturers of new civil supersonic transports are anticipated to use variable noise reduction systems to reduce noise in the vicinity of airports. Certification and implementation considerations unique to these systems are discussed. Characteristics of these systems are likely to require a greater reliance upon system noise modeling and predictions than in the case of conventional subsonic transports. Accurate noise modeling is critical since it would be unfortunate if an applicant designed a noise reduction procedure and built equipment to implement it, only to discover that it did not work as expected during field testing. A novel method for evaluating lateral noise at low altitudes is used to predict performance of a variable noise reduction system for a notional supersonic business jet. A programmed thrust lapse procedure and an automatic flap retraction procedure are found to reduce cumulative certification noise of the transport by an additional 5.2 EPNdB relative to a previous study.

VIII. Acknowledgments

Thanks to NASA's Commercial Supersonic Technology Project for supporting this study. Thanks also go to the International Coordinating Council of Aerospace Industries Associations, particularly GE Aviation and Gulfstream Aerospace Corporation, for their helpful guidance and suggestions. Thanks go to ICAO's Working Group 1 (Aircraft Noise, Technical), and to the FAA, for including supersonic research into their work programs. And special thanks go

to Bruce Conze of the FAA for helping me navigate the complex world of aviation noise standards. The vision of viable supersonic transports operating responsibly in an environmentally sustainable manner is a shared pursuit.

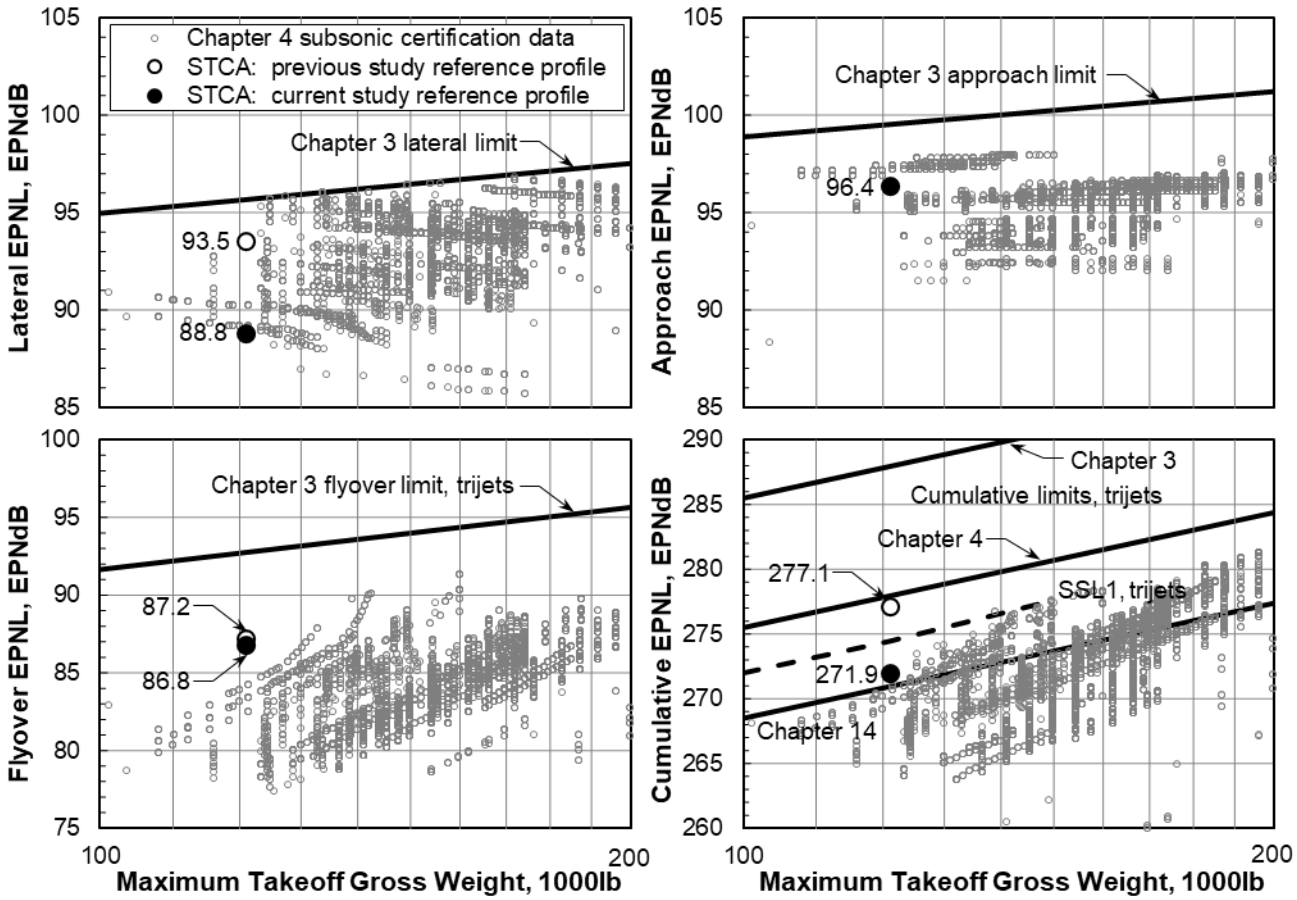

Figure 8. Effective perceived noise level predictions relative to limits and published data.

References

[1] International Civil Aviation Organization: "Development of Supersonic Aeroplanes Subject to Public Acceptability Based on Subsonic Standards," Working Paper 103, Assembly (40th session), presented by Finland, 24 July 2019 [URL: https://www.icao.int/Meetings/a40/Documents/WP/wp_103_en.pdf, retrieved Feb. 2022].

[2] International Civil Aviation Organization: "Views of the United States on Civil Supersonic Flight," Working Paper 261, Assembly (40th session), presented by the United States, 2 Aug. 2019 [URL: https://www.icao.int/Meetings/A40/Documents /WP/wp_261_en.pdf, retrieved Feb. 2022].

[3] Berton, J. J.; Jones, S. M.; Seidel, J. A.; and Huff, D. L., "Noise predictions for a Supersonic Business Jet using Advanced Take-off Procedures," The Aeronautical Journal, Royal Aeronautical Society, Vol. 122 (1250), 2018, pp. 556-571 (doi: 10.1017/aer.2018.6).

[4] Berton, J.; Huff, D.; Seidel, J.; and Geiselhart, K.: "Supersonic Technology Concept Aeroplanes for Environmental Studies," AIAA Paper 2020-0263, AIAA SciTech Forum and Exposition, Orlando, FL, 6-10 Jan, 2020 (doi 10.2514/6.2020-0263).

[5] Rizzi, S.; Berton, J.; and Tuttle, B.: "Auralization of a Supersonic Business Jet Using Advanced Takeoff Procedures," AIAA Paper 2020-0266, AIAA SciTech Forum and Exposition, Orlando, FL, 6-10 Jan, 2020 (doi 10.2514/6.2020-0266).

[6] Nöding, M.; Schuermann, M.; Bertsch, L.; Koch, M.; Plohr, M.; Jaron, R.; and Berton, J.: "Simulation of Landing and Take-off Noise for Supersonic Transport Aircraft at a Conceptual Design Fidelity Level," *MDPI J. Aerospace*, vol. 9, no. 1, 2022 (doi 10.3390/aerospace9010009).

[7] Nöding, M.; and Bertsch, L.: "Application of Noise Certification Regulations within Conceptual Aircraft Design," *MDPI J. Aerospace*, vol. 8, no. 8, 2021 (doi 10.3390/aerospace8080210).

[8] Akatsuka, J.; and Ishii, T.: "System Noise Assessment of NASA Supersonic Technology Concept Aeroplane Using JAXA's Noise Prediction Tool," AIAA paper 2020-0265, 2020 (doi 10.2514/6.2020-0265).
[9] Akatsuka, J.; and Ishii, T.: "Comparative Study of Semi-empirical Jet Noise Prediction Models for Future Commercial Supersonic Aircraft," AIAA paper 2021-2219, 2021 (doi 10.2514/6.2021-2219).
[10] Rutherford, D.; Eastham, S.; Sanz-Morère, I.; Kim, J.; and Speth, R.: "Environmental limits on supersonic aircraft in 2035," International Council on Clean Transportation, Working Paper 2202-02, Jan. 2022 [URL: https://theicct.org/wp-content/uploads/2022/01/aviation-global-supersonic-safs-feb22-1.pdf, retrieved Feb. 2022].
[11] Barrett, S.: "Clean-Sheet Supersonic Aircraft Engine Design and Performance Annual Report," Aviation Sustainability Center (ASCENT) Project 47 Annual Report, Pullman, WA, 2020.
[12] Voet, L.; Prashanth, P.; Speth, R.; Sabnis, J.; Tan, C.; and Barrett, S.: "The impact of Design Space Constraints on the Noise and Emissions from Derivative Engines for Civil Supersonic Aircraft," AIAA paper 2021-1272, 2021 (doi 10.2514/6.2021-1272).
[13] Mavris, D.; Crossley, W.; Tai, J.; and DeLaurentis, D.: "Aircraft Technology Modeling and Assessment," Aviation Sustainability Center (ASCENT) Project 10 Annual Report, Pullman, WA, 2020.
[14] "Environmental Technical Manual, Vol. I, Procedures for the Noise Certification of Aircraft," *International Civil Aviation Organization, Committee on Aviation Environmental Protection*, 2nd ed., Document 9501, 2015.
[15] Federal Aviation Administration: "Noise Standards: Aircraft Type and Airworthiness Certification," Advisory Circular no. 36-4D, 2017.
[16] Berton, J.: "Aircraft Noise and Performance Data for a Notional Supersonic Business Jet," AIAA Paper to be published, 28th AIAA/CEAS Aeroacoustics Conference, Southampton, UK, 14-17 June, 2022.
[17] National Aeronautics and Space Administration, "NASA Awards Contract to Build Quieter Supersonic Aircraft," Press release 18-20, April 2018 [URL: https://www.nasa.gov/press-release/nasa-awards-contract-to-build-quieter-supersonic-aircraft, retrieved Feb. 2022].
[18] Gloudemans, J.; Davis, P.; and Gelhausen, P., "A Rapid Geometry Modeler for Conceptual Aircraft," AIAA-1996-0052, January, 1996 (doi 10.2514/6.1996-52).
[19] Carlson, H. W.; Chu, J.; Ozoroski, L. P.; and McCullers, L. A., "Guide to AERO2S and WINGDES Computer Codes for Prediction and Minimization of Drag Due to Lift," NASA TP-3637, November 1997.
[20] Sommer, S. C. and Short, B. J., "Free-Flight Measurements of Turbulent-Boundary-Layer Skin Friction in the Presence of Severe Aerodynamic Heating at Mach Numbers from 2.8 to 7.0," NACA TN-3391, 1955.
[21] Harris, Roy V., Jr., "An Analysis and Correlation of Aircraft. Wave Drag," NASA TM X-947, 1964.
[22] Wells, D. P.; Horvath, B. L.; and McCullers, L. A., "The Flight Optimization System Weights Estimation Method," NASA TM-2017-219627, vol. 1, 2017.
[23] Phoenix Integration, Inc., ModelCenter, Design Integration Software, 1715 Pratt Drive, Suite 2000, Blacksburg, VA 24060, [URL: http://www.phoenix-int.com, retrieved Feb., 2022].
[24] Geiselhart, K. A.; Ozoroski, L. P.; Fenbert, J. W.; Shields, E. W.; and Wu, L., "Integration of Multifidelity Multidisciplinary Computer Codes for Design and Analysis of Supersonic Aircraft," AIAA Paper 2011-465, 49th AIAA Aerospace Sciences Meeting including the New Horizons Forum and Aerospace Exposition, 4 - 7 January 2011, Orlando, Florida (doi 10.2514/6.2011-465).
[25] Claus, R. W.; Evans, A. L.; Lytle, J. K.; and Nichols, L. D.: "Numerical Propulsion System Simulation," *Computing Systems in Engineering*, Vol. 2, No. 4, 1991, pp. 357-364 (doi 0956-0521/91).
[26] NPSS, Numerical Propulsion System Simulation, Software Package, Ver. 1.6.5, NASA, 2008.
[27] Kirby, M. R.; Mavris, D. N., "The Environmental Design Space," 26th Congress of International Council of the Aeronautical Sciences (ICAS), Anchorage, Alaska, Sep. 14-19, 2008, ICAS 2008-4.7.3.
[28] Nunez, S. L.; Tai, J. C.; and Mavris, D. N.: "The Environmental Design Space: Modeling and Performance Updates." AIAA paper 2021-1422, AIAA SciTech Forum, 2021 (doi:10.2514/6.2021-1422).
[29] Suder, K. L., Prahst, P. S., and Thorpe, S. A., "Results of an Advanced Fan Stage Operating Over a Wide Range of Speed and Bypass Ratio, Part 1: Fan Stage Design and Experimental Results," NASA TM-2011-216769, 2011.
[30] McCullers, L. A., "Aircraft Configuration Optimization Including Optimized Flight Profiles," NASA CP-2327, April 1984, pp. 396-412.
[31] Welge, H. R., et al., "N+2 Supersonic Concept Development and Systems Integration," NASA CR-2010-216842, 2010.
[32] "Annex 16 to the Convention on International Civil Aviation, Vol. I: Aircraft Noise," *International Standards and Recommended Practices – Environmental Protection*, 7th ed., International Civil Aviation Organization, Montreal, July 2014.
[33] "Noise Standards: Aircraft Type and Airworthiness Certification," U.S. Code of Federal Regulations, Federal Aviation Advisory Circular 36-4C, 2003, Title 14, Chap. 1, Part 36.
[34] Petronis, K.: "Applicability of Part 36 to New Supersonic Aircraft," Federal Aviation Administration Memorandum, [URL: https://www.faa.gov/about/office_org/headquarters_offices/agc/practice_areas/regulations/interpretations/Data/interps/2018/Executive_Director-AEE-1_2018_Legal_Interpretation.pdf, retrieved Feb., 2022].

[35] Federal Aviation Administration, "Noise Certification of Supersonic Airplanes," Notice of Proposed Rulemaking, docket no. FAA-2020-0316, notice no. 20-06, 2020 [URL: https://www.federalregister.gov/documents/2020/04/13/2020-07039/noise-certification-of-supersonic-airplanes, retrieved Feb. 2022].
[36] Jackson, E.; Raney, D.; Glaab, L.; and Derry, S.: "Piloted Simulation Assessment of a High-Speed Civil Transport Configuration," NASA TP-2002-211441, 2002.
[37] Foster, C.: "Noise Regulations of the Federal Government," AIAA/SAE 13th Propulsion Conference, AIAA paper 77-995, 1977 (doi 10.2514/6.1977-995).
[38] Grantham, W. D., and Smith, P. M., "Development of SCR Aircraft Takeoff and Landing Procedures for Community Noise Abatement and their Impact on Flight Safety," in *Supersonic Cruise Research*, NASA CP 2108, 1979, pp. 299-333.
[39] Boeing Commercial Airplanes: "High-Speed Civil Transport Study," NASA CR-4233, 1989.
[40] Anon.: "Method for Predicting Lateral Attenuation of Airplane Noise," Soc. of Automotive Engineers SAE-AIR-5662, Warrendale, PA, April 2006.
[41] Anon., "Method for Calculating the Attenuation of Aircraft Ground to Ground Noise Propagation During Takeoff and Landing," Soc. of Automotive Engineers SAE-AIR-923, Warrendale, PA, 1966.
[42] Anon., "Prediction Method for Lateral Attenuation of Airplane Noise During Takeoff and Landing," Soc. of Automotive Engineers SAE-AIR-1751, Warrendale, PA, 1981.
[43] Anon., "Estimation of Lateral Attenuation of Air-to-Ground Jet or Turbofan Aircraft Noise in One-Third Octave Bands," Engineering Science Data Unit Item 82027, ESDU International Plc, London, 1983.
[44] Nicholls, K. P.: "Flap Systems on Supersonic Transport Aircraft," 20th Congress of the International Council of the Aeronautical Sciences, ICAS-96-4.4.4, Sorrento, Napoli, Italy, 8-13 Sept., 1996.
[45] Olson, E.: "Advanced Takeoff Procedures for High-Speed Civil Transport Community Noise Reduction," SAE Transactions, vol. 101, paper no. 921939, SAE International, 1992, pp. 1612-1625.
[46] Business Aviation Insider; "Supersonic Business Jets Are Within Reach," [URL: https://nbaa.org/aircraft-operations/international/supersonic-business-jets-within-reach/, retrieved Feb., 2022].
[47] U.S. Code of Federal Regulations, Title 14, Chap. I, Part 25, Airworthiness Standards: Transport Category Airplanes.
[48] U.S. Code of Federal Regulations, Title 14, Chap. I, Part 91, General Operating and Flight Rules.
[49] "Aircraft Noise and Performance (ANP) Database v2.3," [Online Database], Eurocontrol Experimental Centre, Centre du Bois des Bordes, Brétigny-sur-Orge, France, Oct. 2020, http://www.aircraftnoisemodel.org [retrieved Feb. 2022].
[50] Anon.: "Procedure for the Calculation of Airplane Noise in the Vicinity of Airports," Soc. of Automotive Engineers SAE-AIR-1845, Warrendale, PA, 1995.
[51] Anon.: "Procedure for the Calculation of Airplane Noise in the Vicinity of Airports," Soc. of Automotive Engineers SAE-AIR-1845A, Warrendale, PA, 2012.
[52] Anon.: "Recommended Method for Computing Noise Contours Around Airports," International Civil Aviation Organization Doc. 9911, 2nd ed., Montréal, Quebec, Canada, 2018.
[53] Lee, C., et al.: "Aviation Environmental Design Tool (AEDT) Technical Manual, Version 3b," Federal Aviation Administration DOTVNTSCFAA-19-03, Washington, D.C., Sept. 2019.
[54] Moulton, C. M.: "Air Force Procedure for Predicting Noise Around Airbases: Noise Exposure Model (NOISEMAP)," Rept. AL-TR-1992-0059, Accession no. AD-A255 769, Air Force Systems Command, Wright-Patterson Air Force Base, Dayton, OH, 1992.
[55] Ollerhead, J. B.: "The CAA Aircraft Noise Contour Model: ANCON Version 1," Civil Aviation Authority, Department of Safety, Environment and Engineering, Chief Scientist's Division, Civil Aviation Authority, DORA Rept. 9120, Cheltenham, England, U.K., 1992.
[56] Cavadini, L.: "STAPES (SysTem for AirPort noise Exposure Studies) Final Report," European Aviation Safety Agency Research Project EC TREN/05/ST/F2/36-2/2007-3/S07.77778, Dec. 2009.
[57] Kartyshov, O. A., and Zaporozhets, A. I.: "Metod Rascheta Konturov Aviatsionnogo Schuma [The Method of Calculating Contours of Aircraft Noise]," FGUP GosNI, ZAO TSEB GA, Moscow, 2008.
[58] Zorumski, W. E.: "Aircraft Noise Prediction Program Theoretical Manual, Parts 1 and 2," NASA TM-83199, 1982.
[59] Clark, B. J.: "Computer Program to Predict Aircraft Noise Levels," NASA TP-1913, 1981.
[60] Sahai, A. K., Snellen, M., Simons, D. G., and Stumpf, E., "Aircraft Design Optimization for Lowering Community Noise Exposure Based on Annoyance Metrics," *J. of Aircraft*, Vol. 54, No. 6, 2017, pp. 2257–2269.
[61] Herkes, W. H., and Reed, D. H., "Modular Engine Noise Component Prediction System (MCP) Technical Description and Assessment Document," NASA CR-2005-213526, 2005.
[62] Lopes, L. V., and Burley, C. L.: "Design of the Next Generation Aircraft Noise Prediction Program: ANOPP2," AIAA Paper 2011-2854, June 2011 (doi 10.2514/6.2011-2854).
[63] Anon.: "Gas Turbine Jet Exhaust Noise Prediction," Soc. of Automotive Engineers, SAE-ARP-876, Rev. F, Warrendale, PA, May 2013.
[64] Henderson, B. S.; Huff, D. L.; and Berton, J. J., "Jet Noise Prediction Comparisons with Scale Model Tests and Learjet Flyover Data," AIAA Paper 2019-2768, 25th AIAA/CEAS Aeroacoustics Conference, Delft, Netherlands, 20-23 May, 2019 (doi 10.2514/6.2019-2768).

[65] Henderson, B. S.; and Huff, D. L., "Scale Model Jet Tests for Learjet Flyover Data," oral presentation, AIAA SciTech Forum and Exposition, 6-10 January, 2020.
[66] Bridges, J.; and Wernet, M.: "Noise of Internally Mixed Exhaust Systems With External Plug For Supersonic Transport Applications," AIAA Paper 2021-2218 (doi 10.2514/6.2021-2218).
[67] Cluts, J.; Bridges, J.; and Podboy, G.: "Translating Phased Array Measurements of a Low-Noise Top-Mounted Propulsion Installation for a Supersonic Airliner," AIAA Paper 2019-0251 (doi 10.2514/6.2019-0251).
[68] Bridges, J.; and Wernet, M.: "PIV measurements of a low-noise top-mounted propulsion installation for a supersonic airliner," AIAA Paper 2019-0252 (doi 10.2514/6.2019-0252).
[69] Bridges, J.; Zaman, K.; and Heberling, B.: "Basics of Mixer-Ejectors for Quiet Propulsion," AIAA Paper 2020-2505 (doi 10.2514/6.2020-2505).
[70] Kontos, K. B., Janardan, B., and Gliebe, P. R., "Improved NASA-ANOPP Noise Prediction Computer Code for Advanced Subsonic Propulsion Systems, Volume 1: ANOPP Evaluation and Fan Noise Model Improvement," NASA CR-195480, 1996.
[71] Hough, J. W.; and Weir, D. S., "Aircraft Noise Prediction Program (ANOPP) Fan Noise Prediction for Small Engines," NASA CR-198300, 1996.
[72] Woodward, R. P.; Gazzaniga, J. A.; and Hughes, C. E., "Far-Field Acoustic Characteristics of Multiple Blade-Vane Configurations for a High Tip Speed Fan," NASA TM-2004-213093, May 2004.
[73] Weir, D. S., "Design and Test of Fan/Nacelle Models Quiet High-Speed Fan," NASA CR-2003-212370, July 2003.
[74] Kontos, K. B.; Kraft, R. E.; and Gliebe, P. R., "Improved NASA-ANOPP Noise Prediction Computer Code for Advanced Subsonic Propulsion Systems, Volume 2: Fan Suppression Model Development," NASA CR-202309, 1996.
[75] Emmerling, J. J., Kazin, S. B., and Matta, R. K., "Core Engine Noise Control Program. Vol. III, Supplement 1-Prediction Methods," FAA RD-74-125, III-I, March 1976.
[76] Fink, M. R., "Airframe Noise Prediction Method," FAA RD-77-29, March 1977.
[77] Herkes, W. H.; Stoker, R. W., "Wind Tunnel Measurements of the Airframe Noise of a High-Speed Civil Transport," AIAA Paper A98-16338, 36th Aerospace Sciences Meeting and Exhibit, Reno, NV, 12-15 January, 1998 (doi 10.2514/6.1998-472).
[78] Rawls, J. W.; and Yeager, J. C., "High Speed Research Noise Prediction Code (HSRNOISE) User's and Theoretical Manual," NASA CR-2004-213014, 2004.
[79] Maekawa, Z., "Noise Reduction By Screens," *Memoirs of the Faculty of Engineering,* Vol. 12, Kobe Univ., Kobe, Japan, 1966, pp. 472–479 (doi 10.1016/0003-682X(68)90020-0).
[80] Anon.: "Standard Values of Atmospheric Absorption as a Function of Temperature and Humidity," Soc. of Automotive Engineers, SAE-ARP-866A, Warrendale, PA, 1975.
[81] Chien, C F..; and Soroka, W. W.; "Sound propagation along an impedance plane," *J. Sound and Vibration*, 1975, 43, (1), pp 9-20 (doi 10.1016/0022-460X(75)90200-X).
[82] Chien, C. F., and Soroka, W. W., "A Note on the Calculation of Sound Propagation Above an Impedance Surface," *J. Sound and Vibration,* vol. 69, no. 2, 1980, pp. 340-343 (doi 10.1016/0022-460X(80)90618-5).
[83] Embleton, T. F. W.; Piercy, J. E.; and Daigle, G. A.; "Effective flow resistivity of ground surfaces determined by acoustical measurements," *J. Acoustical Society of America*, 1983, 74, (4), pp 1239-1244 (doi 10.1121/1.390029).
[84] Willshire, W.L.: "Assessment of Ground Effects on the Propagation of Aircraft Noise: The T-38A Flight Experiment," NASA TP-1747, 1980.
[85] Plotkin, K. J.; Hobbs, C. M.; and Bradley, K. A.: "Examination of the Lateral Attenuation of Aircraft Noise," NASA CR-2000-210111, 2000.
[86] Berton, J.: "Simultaneous use of Ground Reflection and Lateral Attenuation Noise Models," *Journal of Aircraft,* vol. 59, no. 2, 2022, pp. 536-543 (doi 10.2514/1.C036488).
[87] Kirby, M. R.; and Mavris, D. N.: "Noise-Power-Distance Re-Evaluation Annual Report," Aviation Sustainability Center (ASCENT) Project 43 Annual Report, Pullman, WA, 2020.
[88] Berton, J.: "Simultaneous use of Ground Reflection and Lateral Attenuation Noise Models," AIAA paper, 2021-2214 (doi 10.2514/6.2021-2214).
[89] Voet, L.; Speth, R.; Sabnis, J.; Tan, C.; and Barrett, S.: "Towards the Design of Variable Noise Reduction Systems for Civil Supersonic Transport Take-off Certification Noise Reduction," AIAA Paper to be published, 28th AIAA/CEAS Aeroacoustics Conference, Southampton, UK, 14-17 June, 2022.
[90] Voet, L.; Speth, R.; Sabnis, J.; Tan, C.; and Barrett, S.: "Sensitivities of Aircraft Acoustic Metrics to Engine Design Variables for Multi-disciplinary Optimization," *AIAA Journal* article accepted for publication, to be published 2022.
[91] Murphy, B.: "Sustainable Supersonics: An Industry Perspective," Boom Technology slide presentation, Environmental Impact of Supersonic Transports Workshop, AIAA SciTech Forum, 4 Jan. 2022.
[92] FAA Docket No. NM248; Special Conditions No. 25-241-SC, "Special Conditions: Embraer Model ERJ-170 Series Airplanes; Electronic Flight Control Systems; Automatic Takeoff Thrust Control System," 5 Sept. 2003.
[93] FAA Docket No. NM26; Special Conditions No. 25-ANM-23, "Special Conditions: Airbus Industrie Model A320 Series Airplane," 15 Dec. 1988.

[94] Guynn, M.; Berton, J.; Tong, M.; and Haller, W.: "Advanced Single-Aisle Transport Propulsion Design Options Revisited," AIAA Paper 2013-4330, 2013 (doi 10.2514/6.2013-4330).
[95] Csank, J.; and Thomas, G.: "Dynamic Analysis for a Geared Turbofan Engine with Variable Area Fan Nozzle," AIAA paper 2017-4819, 2017 (doi 10.2514/6.2017-4819).
[96] Morgenstern, J.; Norstrud, N.; Sokhey, J.; Martens, S.; and Alonso, J.: "Advanced Concept Studies for Supersonic Commercial Transports Entering Service in the 2018 to 2020 Period, Phase I Final Report," NASA CR-2013-217820, 2013.
[97] International Civil Aviation Organization: "Supersonic Exploratory Study Report," Committee on Aviation Environmental Protection, Steering Group meeting (virtual), Information Paper 3, presented by the Supersonic Coordination Group Focal Point, 5-16 Jul. 2021.
[98] International Civil Aviation Organization: "Supersonic Exploratory Study Report," Committee on Aviation Environmental Protection, Steering Group meeting (virtual), Working Paper 31, presented by the Supersonic Coordination Group Focal Point, 5-16 Jul. 2021.
[99] International Civil Aviation Organization: "Views of the United States on Supersonic Aircraft Noise Future Work during the CAEP/13 Cycle," Committee on Aviation Environmental Protection (12th meeting), Working Paper 64, presented by the United States, 17-18 Feb. 2022 [URL: https://icao.usmission.gov/wp-content/uploads/sites/280/CAEP.12.WP_.064.16.en-VIEWS-OF-THE-UNITED-STATES-ON-SUPERSONIC-AIRCRAFT-NOISE-FUTURE-WORK-DURING-THE-CAEP13-CYCLE.pdf, retrieved Feb. 2022].
[100] International Civil Aviation Organization: "Proposal for Supersonic LTO Noise SARP in CAEP/13 Future Work Programme," Committee on Aviation Environmental Protection, Working Group 1 (Noise, Technical), 8th meeting (virtual), Working Paper 15, presented by the International Coordinating Council of Aerospace Industries Associations and the International Business Aviation Council, 27-30 Sept. 2021.